



ELSEVIER

Contents lists available at ScienceDirect

Journal of Combinatorial Theory, Series A

www.elsevier.com/locate/jcta



Blossoming bijection for higher-genus maps



Mathias Lepoutre¹

LIX, École polytechnique, 1 rue Honoré d'Estiennes d'Orves, 91120 Palaiseau, France

ARTICLE INFO

Article history:
Received 7 June 2018
Available online xxxx

Keywords:
Combinatorics
Bijection
Maps
Higher genus
Blossoming tree
Rationality

ABSTRACT

In 1997, Schaeffer described a bijection between Eulerian planar maps and some trees. In this work we generalize his work to a bijection between maps on an orientable surface of any fixed genus and some unicellular maps with the same genus. An important step of this construction is to exhibit a canonical orientation for maps, that allows to apply the same local opening algorithm as Schaeffer did.

As an important byproduct, we obtain the first bijective proof of a result of Bender and Canfield from 1991, when they proved that the generating series of maps in higher genus is a rational function of the generating series of planar maps.

© 2019 Elsevier Inc. All rights reserved.

1. Introduction

A *map* of genus g is a proper embedding of a graph in \mathbb{S}_g , the torus with g holes. In addition to be rich combinatorial objects by themselves, maps have many links with various fields of algebra and mathematical physics (*e.g.* [24,19]). The probabilistic approach of maps, leading to the definition of continuous surfaces such as the Brownian map, is also a very active domain. The structural study of maps is a deep subject, and

E-mail address: mathias.lepoutre@polytechnique.edu.

¹ Partially supported by the project ANR-16-CE40-0009.

it seems that it is always interesting to have a better understanding of maps, given the very diverse related topic.

Planar maps (or maps of genus 0) have been studied extensively since the pioneering work of Tutte in the sixties [30]. In a series of work, Tutte obtained remarkable formulas for many families of maps. His techniques rely on some recurrence relations for maps, obtained through combinatorial decomposition, and some clever manipulations of generating series. They were extended in the late eighties to the case of maps with higher genus by Bender and Canfield, who first obtained the asymptotic number of maps on any orientable surface of genus g [4] and then obtained in [2] in 1991 the following stronger result:

Theorem 1.1 (Bender and Canfield [2]). *For any $g \geq 0$, the generating series $M_g(z)$ of maps of genus g enumerated by edges is a rational function of z and $\sqrt{1 - 12z}$.*

The enumerative results obtained using Tutte’s techniques show some underlying very strong structural properties of maps, and call for bijective explanations. The first such explanation was the bijection of Cori and Vauquelin [17]. Indeed, the enumerative formula of planar maps obtained by Tutte has a very simple closed form, that Cori and Vauquelin were the first to explain bijectively in 1981. This work was soon followed by many others, starting with the pioneering work of Schaeffer, in the late 90s, and was the beginning of the bijective combinatorics of maps.

In this vein, the purpose of this paper is to give a bijective explanation of enumerative results in higher genus. In particular, our main result is the first bijective proof of Theorem 1.1, for $g \geq 2$.

In the planar case, Schaeffer exhibits in [28] a constructive bijection between Eulerian planar maps and some so-called *blossoming trees*. The blossoming tree associated to a map is one of its spanning trees, decorated by some *stems*, that enable to reconstruct the “missing edges”. Our work is a generalization of [28] to maps of any genus.

In genus $g > 0$, the natural counterpart of trees are unicellular maps (*i.e.* maps with only one face) and we obtain in this work the following result (the terminology is introduced in Section 3.3):

Theorem 1.2. *There exists a constructive weight-preserving and genus-preserving bijection between rooted bicolored maps and well-rooted well-labeled well-oriented unicellular blossoming maps.*

Thanks to this theorem, the enumeration of maps boils down to the much easier enumeration of this specific family of unicellular blossoming maps. Using techniques used in particular by Chapuy, Marcus, and Schaeffer in [16], we are able to decompose these unicellular maps into a *scheme* with *branches*. Similarly to [16], the proof of Theorem 1.1 then amounts to showing a certain symmetry, that we are able to prove.

Let us now put our work in context of the existing literature. In the planar case, there are numerous bijections between maps and some families of decorated trees. Two main

trends emerge in these bijections. Either the decorated trees are some blossoming trees as already described (*e.g.* [17,28,11,26]) or the trees are decorated by some integers that capture some metric properties of the maps (*e.g.* [29,12]). Bijections of the latter type have been successfully extended to higher genus [16,14,25], and to non-orientable surfaces ([15,9]). These techniques (in particular, see [16]), exhibit a decomposition (which is known to be rational by Theorem 1.1) of maps into trees. This allows to show in a bijective way that the generating series of maps can be expressed as a rational function of some auxiliary functions U , whose degree of algebraicity is just higher than the enumerative results of Theorem 1.1. Note however that, in the case $g = 1$, Chapuy Marcus and Schaeffer [16] were able to carry on the calculation and give a bijective proof of Theorem 1.2.

The situation is different in the case of bijections with blossoming trees. As demonstrated by Bernardi [5] in the planar case and generalized by Bernardi and Chapuy [6], a map endowed with an orientation of its edges with specific properties can also be viewed (by what can be seen as an opening algorithm) as a map endowed with a spanning unicellular embedded graph (whose genus can be smaller than the genus of the initial surface). This generalizes blossoming bijections to a broader setup where maps come with an orientation, even though the genus of the resulting map is not fixed. To obtain a bijective scheme starting from non-oriented maps, the common strategy will be to find a good way to define a canonical orientation, apply the opening algorithm, and prove that the resulting has the correct genus. This has been done in genus 1 in several recent works; [18] presents a bijection for simple triangulations of genus 1 (with some additional constraints), while [10] presents a bijection for essentially 4-connected triangulations. However, our work, which generalizes [28], is the first blossoming bijection that applies to maps in any genus.

In the planar case, the general theory of α -orientations developed by Felsner [20] has been successfully combined with the result of [5] to give general bijective schemes [7,8,1], which enable to recover the previously known bijections. It would be highly desirable to obtain systematic bijective schemes in higher genus by combining Bernardi and Chapuy's result together with the theory of c -orientations introduced by Propp [27] or its extension by Felsner and Knauer [21]. The main difficulty to tackle would be to characterize the orientations that produce spanning unicellular embedded graph whose genus matches the genus of the original surface. The orientation we choose in our work does produce such embedded graphs, and our work can hence be seen as an important step in that direction.

The bijection of Schaeffer [28] for Eulerian maps was extended by Bouttier, di Francesco and Guitter [11] to general maps. This work was then revisited by Albenque and Poulhalon [1], whose general framework allows to see the bijection of [11] as the opening of a map, endowed with a well-chosen fractional orientation. In Section 6, we generalize these extensions to maps on surfaces of any genus, so as to get a direct bijection between general maps and some unicellular blossoming maps.

Our main result deals with the rationality of bicolored 4-valent maps. It would be very interesting to have similar rationality results for general bicolored maps, with a control on the degrees of the vertices, for instance by giving a rational parametrization of bicolored maps of degree at most 6. We plan to explore this direction in future work.

In [3], Bender, Canfield and Richmond generalized the work of [2], by enumerating maps by vertices and faces instead of edges only. Similarly, they prove the existence of a rational parametrization of the generating series in higher genus. It would be really interesting to generalize our work so as to obtain a combinatorial explanation of this more general rational parametrization. This is another direction that we wish to explore in future work.

To conclude, note that there are a lot of other more precise structural or enumerative properties of maps and related objects that can be proved using involved mathematical studies and calculations. For instance, Carrell and Chapuy [13] were able to give many recurrence formulas for maps in any genus, and their generating functions, while Eynard [19] uses the so-called “random matrix method” to perform the enumeration of maps. These results (and others), which are often way more precise than the rationality of generating functions, still call for bijective or combinatorial explanations.

Organization of the paper: In Section 2, we recall definitions about maps and orientations and state Propp’s theorem adapted to our setting. In Section 3, we define an explicit and constructive bijection between (4-valent or not) bicolored maps and a family of unicellular maps. In Section 4, we analyze this family by reducing these maps to schemes, reducing the proof of Theorem 1.1 to the rationality of a restricted family of maps, that all have the same *scheme*, or alternatively, the symmetry of this series in terms of an intermediate series. In Section 5 we prove this symmetry by doing some additional work based on surjections. Finally in Section 6 we present an extension of our main bijection to general maps (not necessarily bicolored), using fractional orientations.

Notation: In this article, combinatorial families are named with calligraphic letters, their generating series is the corresponding capital letter, and an object of the family, is usually denoted by the corresponding lower case letter. The size being denoted by $|\cdot|$, we therefore have for a combinatorial family \mathcal{S} : $S(z) = \sum_{s \in \mathcal{S}} z^{|s|}$.

2. Orientations in higher genus

2.1. General

We begin with some definitions about maps.

Definition 2.1 (*Embedded graph, map*). An *embedded graph* is an embedding of a connected graph into a given compact surface, taken up to orientation-preserving homeomorphisms of the surface. An embedded graph is *cellularly embedded* if all its *faces*

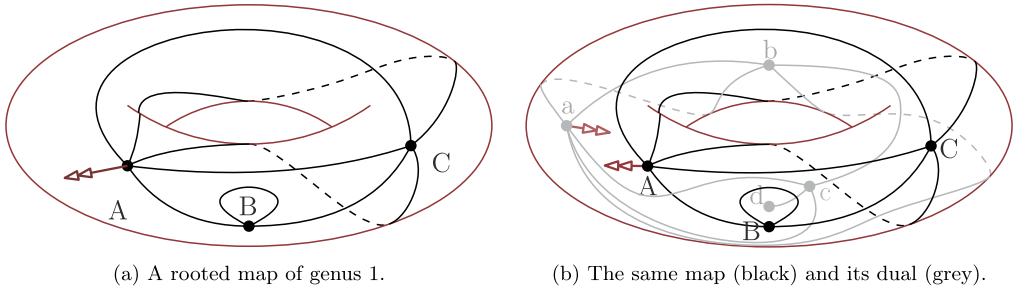


Fig. 1. Examples of maps. The root corner is indicated by a double-arrow.

(connected component of the complement) are homeomorphic to discs. A *map* is a cellularly embedded graph.

The set of maps, counted by number of edges, is denoted \mathcal{M} . In this paper we only consider maps embedded on orientable surfaces. *General maps* have no other restriction, and in particular, can have loops or multiple edges.

A map on an orientable surface can alternatively be defined as a graph equipped with a cyclic order on edges around each vertex, or as a gluing of polygons.

Note that if a graph is non-cellularly embedded, its face might be surfaces with any genus and any positive number of borders.

Definition 2.2 (Genus). The *genus* of a map is the genus of its underlying surface.

The genus of an embedded graph is the genus of the map obtained by replacing each border of each face of the embedded graph by a disk.

Since any face of an embedded graph has a positive number of borders, the genus of an embedded graph is lower or equal to the genus of its underlying surface. All families of maps can be refined by their genus; we denote this refinement by an index indicating the topological genus, so that for instance \mathcal{M}_0 is the set of maps in the sphere. See Fig. 1a for an example of map of genus 1.

Definition 2.3 (Corner, degree). An adjacency between a face and a vertex is called a *corner*. Note that a single pair vertex-face can give rise to several distinct corners. The *degree* of a face (resp. vertex) is the number of adjacent corners.

Definition 2.4 (Rooting). A map is said to be *rooted* if one of its corners, called the *root corner* (indicated by a brown arrow in the pictures), is distinguished. The vertex and face adjacent to the root corner are called *root vertex* and *root face*.

Because they may have non-trivial automorphisms, the enumeration of non-rooted maps is difficult. Rather, from now on, we choose to always consider rooted map.

The set of vertices (resp. edges, faces) of a map $m \in \mathcal{M}$ is denoted $\mathcal{V}(m)$ (resp. $\mathcal{E}(m)$, $\mathcal{F}(m)$). The number of vertices (resp. edges, faces) of m is denoted $v(m)$ (resp. $e(m)$, $f(m)$). These notations can also be specified by degree, so that for instance $f_k(m)$ is the number of degree- k -faces of m . The genus of m is denoted $g(m)$. We recall Euler’s formula:

Proposition 2.5 (Euler’s formula). *For any map $m \in \mathcal{M}$, $v(m) - e(m) + f(m) = 2 - 2g(m)$.*

Definition 2.6 (Dual map). Since an edge connects two vertices and separates two faces, we can define the *dual map* m^* of m by exchanging the role of vertices and faces, and swapping the connection and separation induced by each edge (see Fig. 1b). The root corner remains the same (but its vertex and its face are exchanged).

Note that duality is involutive: $(m^*)^* = m$.

Definition 2.7 (Unicellular, tree). An embedded graph is called *unicellular* if it has only one face. A *tree* is an embedded graph with no cycle.

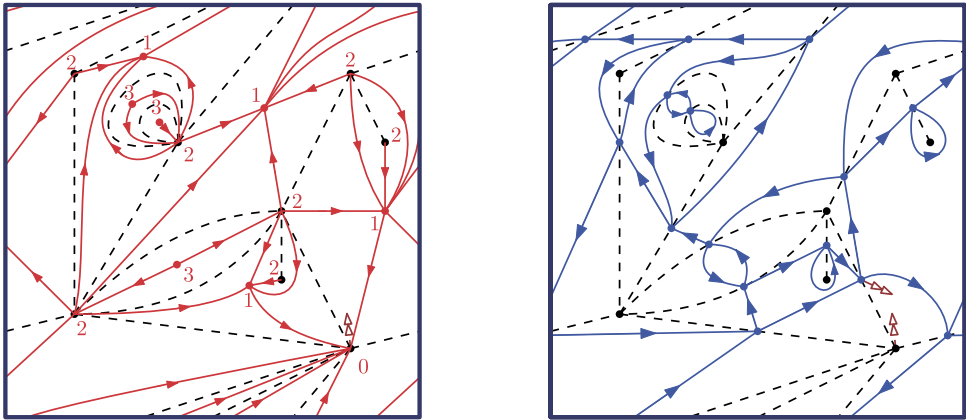
Trees are unicellular and have genus 0. Note that in genus 0, any unicellular embedded graphs is a tree, whereas in a positive-genus surface, a unicellular embedded graph may have any genus lower than the genus of the surface.

Definition 2.8 (Bipartite map, bicolorable map). A map is *bipartite* if its underlying graph is bipartite, which means that its vertices can be *properly* (so that no 2 adjacent vertices have same color) colored black and white. Dually, a map is *bicolorable* if its faces can be *properly* (so that no 2 adjacent faces have same color) colored black and white.

Note that in particular, a bipartite map has no loop. Note also that the faces of a bipartite map and the vertices of a bicolorable map necessarily have even degree. The set of bipartite (resp. bicolorable) maps counted by number of faces (resp. vertices) is denoted \mathcal{BP} (resp. \mathcal{BC}). The generating series of bipartite and bicolorable maps, $BP(z)$ and $BC(z)$, can be refined in the following way:

$$\begin{aligned}
 BP(\mathbf{z}) &= BP(z_1, z_2, \dots) = \sum_{m \in \mathcal{BP}} \prod_{k=1}^{\infty} z_k^{f_{2k}(m)} \stackrel{\text{duality}}{=} \sum_{m \in \mathcal{BC}} \prod_{k=1}^{\infty} z_k^{v_{2k}(m)} \\
 &= BC(z_1, z_2, \dots) = BC(\mathbf{z}).
 \end{aligned}
 \tag{1}$$

Remark 2.1. A map is called *Eulerian* if all its vertices have even degree. Note that bicolorable maps are Eulerian, and in fact the notions are equivalent in genus 0. However this is not the case in higher genus, where some additional non-local constraints appear along non-contractible cycles. Though Eulerian is a more common property for graph, it seems that, in our setup, bicolorability is a more relevant map property, in particular in view of Proposition 2.10.



(a) A map (dashed black) with its (bipartite quadrangulation) quadrangulated map (full red), with geodesic orientation.

(b) A map (dashed black) with its (4-valent bicolorable) radial map (full blue), with dual-geodesic orientation.

Fig. 2. Classical constructions on a toroidal map. (For interpretation of the colors in the figure(s), the reader is referred to the web version of this article.)

Definition 2.9 (*Quadrangulation, 4-valent map*). A map is called a *quadrangulation* if all its faces have degree 4. Dually, a map is *4-valent* if all its vertices are of degree 4.

The set of bipartite quadrangulations (resp. bicolorable 4-valent maps), counted by number of faces (resp. number of vertices), is denoted \mathcal{BP}^\square (resp. \mathcal{BC}^\times). Their generating series therefore satisfy: $BP^\square(z) = BP(0, z, 0, 0, \dots) \stackrel{\text{duality}}{=} BC(0, z, 0, 0, \dots) = BC^\times(z)$.

Proposition 2.10 (*Folklore*). General maps of genus g with n edges are in bijection with 4-valent bicolorable maps of genus g with n vertices, or dually, with bipartite quadrangulations of genus g with n faces. Therefore, $M_g(z) = BC_g^\times(z) = BP_g^\square(z)$.

Proof. Starting from a map m , we construct bijectively as follows a 4-valent bicolorable map called the *radial map* and denoted r . We create a vertex in r for each edge of m . For each corner of m , we then add an edge in r between the two vertices corresponding to the edges of m adjacent to the chosen corner. Out of the two corners of r corresponding to the root corner of m , we choose the leftmost one as the root corner of r . See Fig. 2b for an example (the orientation of the edges will be explained in Section 2.2). \square

Note that the radial map is the dual of the so-called *quadrangulated map* (see Fig. 2a).

2.2. Structure of orientations of a graph

Definition 2.11 (*Orientation, dual orientation*). An *orientation* of a map is an orientation of each of its edges. The *dual orientation* o^* of an orientation o of a map m is the

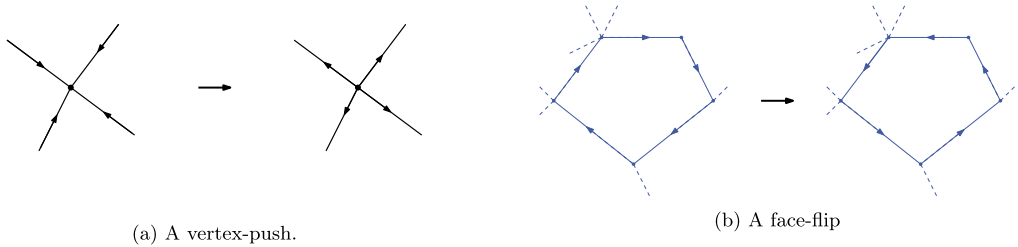


Fig. 3. Some operations on orientations of maps.

orientation of m^* where all dual edges are oriented from the face to the right of the primal edge toward the face to its left.

Note that applying duality twice reverses the orientation (duality on oriented maps is not involutive).

Orientations provide additional structural properties to maps, useful for algorithmic purposes. However, since our final purpose is to study maps without an orientation, it is convenient to assign a canonical orientation to maps. Such an orientation will be provided in Corollary 2.19, and will be obtained as the minimum of a lattice of orientations, as described below.

Definition 2.12 (*Bipartite orientation, vertex-push*). An orientation of a map is called *bipartite*, if it has as many forward edges as backward edges along any cycle (note that any cycle of a bipartite map is made of an even number of edges). The set of bipartite orientations is endowed with the *vertex-push* operation (see Fig. 3), that changes a sink distinct from the root into a source, by reversing all adjacent edges.

A map that has a bipartite orientation is necessarily bipartite.

Definition 2.13 (*Bicolorable orientation*). An orientation of a map is called *bicolorable* if its dual orientation is bipartite.

In other words, each dual cycle has as many edges crossing to the right as edges crossing to the left. A map that has a bicolorable orientation is necessarily bicolorable.

Remark 2.2. This definition is reminiscent to some other works on orientations of maps on the torus [23]. Here, however, it works in any genus.

Remark 2.3. A bicolorable orientation is Eulerian, meaning that all vertices have equal indegree and outdegree. However, again, the 2 notions are not equivalent on a surface of positive genus, but this is not only due to Remark 2.1: even if the map is bicolorable, an Eulerian orientation is not necessarily bicolorable, because of the existence of some non-contractible dual cycles inducing additional non-local constraints for bicolorability of the orientation.

Definition 2.14 (*Face-flip*). The set of bicolored orientations is endowed with the operation dual to vertex push, called the *face-flip*.

Remark 2.4. Face-flips can alternatively be defined in the following way (see Fig. 3b): take a clockwise face distinct from the root, and change the orientation of all edges adjacent to that face.

Vertices of a bipartite map can be labeled by their distance to the root. Since the map is bipartite, two adjacent vertices cannot have the same label.

Definition 2.15 (*Geodesic orientation, dual-geodesic orientation*). The *geodesic orientation* of a bipartite rooted map is the orientation whose edges are all oriented towards their extremity with smaller label.

The dual of the geodesic orientation is called the *dual-geodesic orientation* (see Fig. 2b for an example).

Along any cycle, forward (resp. backward) edges in the geodesic orientation correspond to a label increasing (resp. decreasing) by exactly 1. Therefore, the geodesic orientation is bipartite, and the dual-geodesic orientation is bicolored.

The next result directly follows from [27, Theorem 1].

Theorem 2.16 (*Propp*). *The transitive closure of the vertex-push operation endows the set of bipartite orientations of a fixed bipartite map with a structure of distributive lattice.*

In particular, this means that this set has a unique minimum for vertex-push. By definition, the only sink of the geodesic orientation is the root vertex, which means that the geodesic orientation is minimal for the vertex-push operation, and by consequence:

Corollary 2.17. *The minimum of the above-mentioned lattice of bipartite orientation of a map is the geodesic orientation of this map.*

Furthermore, we obtain by duality:

Corollary 2.18. *The transitive closure of the face-flip operation endows the set of bicolored orientations of a fixed bicolored map with a structure of distributive lattice, and its minimum is the dual-geodesic orientation.*

We can therefore characterize uniquely the dual-geodesic orientation of a given bicolored map:

Corollary 2.19. *The dual-geodesic orientation of a bicolored map is the unique bicolored orientation of this map with no clockwise face other than the root face.*

Remark 2.5. In recent attempts to extend orientations on maps of higher genus, the notion of α -orientations, due to Felsner [20], has been used (*e.g.* in [23]). This leads to study Eulerian orientations (see Remark 2.3) instead of bicolorable orientations.

Unfortunately, Eulerian orientation with the face-flip operation gives rise to several unconnected lattices. A classical approach would be to canonically select one of these connected components, and only work on this one. A natural choice for such a component is the set of bicolorable orientations, which are indeed a strict subset of Eulerian orientation. Therefore, defining bicolorable orientations in the first place seems more convenient for our purposes.

In the rest of this paper, we will use orientation of maps as an additional layer of information, useful for algorithmic purposes, but determined in a canonical way using Corollary 2.19.

3. Closing and opening maps

In this section, we describe an algorithm called the *opening algorithm*, that starts from an oriented map, and, if the orientation respects certain conditions, creates a unicellular blossoming map whose *closure* is the original map. The first version of this algorithm was described by Schaeffer in [28] and amounts to the opening of Eulerian planar maps with a canonical orientation. It was then generalized by Bernardi in [5], and Bernardi and Chapuy in [6] for the higher-genus case, to the general case of a map with an orientation.

The present work, however, is a direct generalization of [28], and we use the usual strategy of choosing a canonical orientation for each map. It is a particular case of [6] in which we are able to go further in the analysis. See Remark 3.5 for a more detailed discussion of the links between the two approaches.

3.1. Blossoming maps and their closure

Definition 3.1 (*Blossoming map, bud, leaf*). A *blossoming map* b is a map with additional stems attached to its corners. These stems are oriented and hence can be of two types; an outgoing stem is called a *bud*, while an ingoing stem is called a *leaf*. We require that a blossoming map has as many buds as leaves. Blossoming maps are always assumed to be rooted on a bud.

Definition 3.2 (*Interior map*). The *interior map* of a blossoming map b , denoted b° , is the map obtained from b by removing all its stems.

Most blossoming maps we usually consider are oriented, which leads to these additional definitions:

Definition 3.3 (*Blossoming degrees*). In a blossoming oriented map, the *interior degree* (resp. *blossoming degree*, resp. *degree*) of a vertex is the degree of this vertex in the

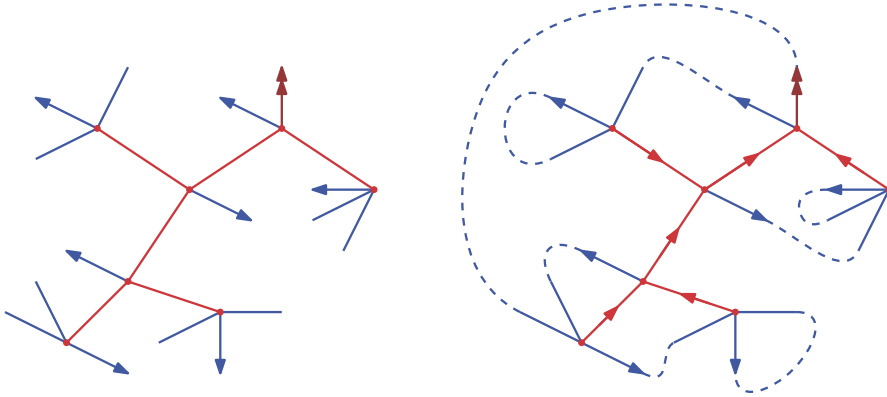


Fig. 4. The closure of a (well-rooted) blossoming tree.

interior map (resp. the number of stems attached to it, resp. the sum of the interior and blossoming degrees). These can all be refined into *ingoing* and *outgoing* degrees.

As stated in Theorem 1.2, unicellular blossoming maps are instrumental to our approach, because they can encode maps, while being easier to analyze. To describe the bijection mentioned in Theorem 1.2, called the *closing algorithm*, we first introduce the *contour word* of a blossoming unicellular map.

Definition 3.4 (*Contour word*). Let b be a blossoming unicellular map. The *contour word* of b is the word on 2 letters U and D defined as follows: when doing a clockwise tour of the unique face (which means that the face is on the right), starting from the root bud, write U (for up-step) for each bud and D (for down-step) for each leaf. The contour word can naturally be seen as a 1-dimensional walk with up- and down-steps, starting and ending at height 0.

We describe in Algorithm 1 how a unicellular blossoming map can be *closed* into a general map (see Fig. 4 for a planar example, and Fig. 7 from right to left for a genus-1 example). The result of the closing algorithm applied to a map b is called the *closure* of b and denoted $Close(b)$.

Algorithm 1 The closing algorithm.

Let b be a unicellular blossoming map.

We write the contour word of b and match its steps by pairs upstep/downstep: each up-step U going from height i to $i + 1$ is matched to the first down-step D after U going from height $i + 1$ to i .

This is done in a cyclic manner, meaning that if there is no downstep going from height $i + 1$ to height i after the last upstep of the contour word going from height i to height $i + 1$, then this last upstep is to be matched with the first downstep going from height $i + 1$ to height i , whose existence is assured by the fact that the contour word ends at height 0.

The stems corresponding to matched steps are then merged into a single oriented edge.

The new map is rooted on the corner just on the right of the edge formed by the former root bud, around the root vertex.

Note that the way stems are matched, which is similar to a well-parenthesizing matching, implies that the created edges are non-crossing. Note also that the cyclic definition of the closing algorithm means that the matching does not depend on the root. This implies that several blossoming unicellular maps can lead to the same map, up to the position of the root. However this is not the case anymore if we restrict the way a blossoming map can be rooted.

Definition 3.5 (*Well-rooted*). A map b is called *well-rooted* if its contour word is a Dyck word.

Remark 3.1. When applying the closing algorithm to a well-rooted map, since the contour word is a Dyck path, the cyclic definition of the algorithm is not needed, which implies that all closing edges have the root on their right.

Definition 3.6 (*Rootable stem, drifted contour word, well-rootable stem*). A stem is called *rootable* if it is either a leaf or the root bud.

The *drifted contour word* of a map b is obtained from its contour word by changing the root up-step into a down-step. The drifted contour word goes from height 0 to height -2 , and its minimum height is denoted $-k$.

The first step going from height $-k + 2$ to height $-k + 1$ and the first step going from height $-k + 1$ to height $-k$ (and the corresponding stems) are called *well-rootable steps/stems*.

Note that well-rootable stems are rootable, and that if we apply a cyclic permutation to a drifted contour word, the well-rootable steps remain the same.

Remark 3.2. A map b is well-rooted if and only if its root bud is well-rootable.

Definition 3.7 (*Undirected map, root-equivalence, unrooted map*). The *undirected map* of a blossoming map is the map obtained by forgetting the orientation of both the edges and the stems.

Two rooted blossoming unicellular maps are called *root-equivalent* if they have the same undirected map and the same set of rootable stems (in particular they do not necessarily have the same root).

The *unrooted map* \bar{b} of b is the equivalence class of b for root-equivalence.

Remark 3.3. By definition, \bar{b} contains the information of which stems are rootable. Hence, the blossoming orientation of b can be fully recovered from \bar{b} if we know which rootable stem of \bar{b} is the root of b .

Remark 3.4. Note that two root-equivalent map have the same well-rootable stems, so that it is possible to distinguish which rootable stems of an unrooted map are well-rootable. As a consequence, a well-rooted map can alternatively be seen as unrooted

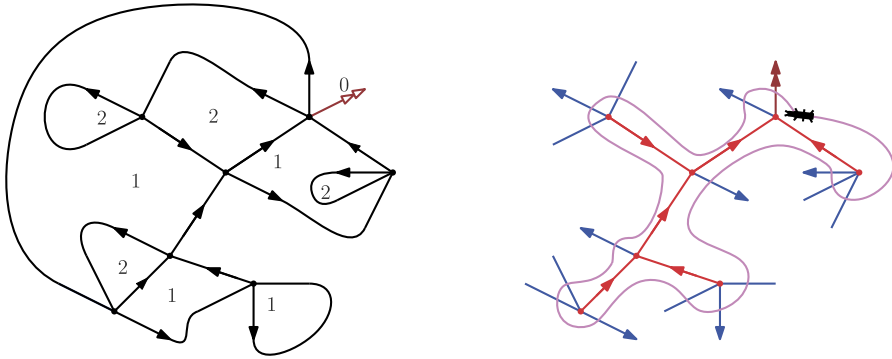


Fig. 5. The opening of a planar map with dual-geodesic orientation.

map with a distinguished well-rootable stem. This point of view will be useful in Section 4.1.

3.2. The opening algorithm

Given a rooted oriented map m , we describe the *opening algorithm* as follows (a more rigorous description will be given later in Algorithm 2). We explore the map starting from the root. When we meet an unexplored edge, if it is ingoing, we follow it, if it is outgoing, we cut it and replace it by a bud. When we meet an already explored edge, it was either followed, in which case we follow it back, or cut, in which case we just add a leaf. We stop when we get back to the root. The resulting blossoming map is called the *opening* of m and denoted $Open(m)$. A planar example of an execution of the opening algorithm is given in Fig. 5, and a genus-1 example is given in Fig. 7, from left to right.

More formally, we define the algorithm as a walk in the *corner map*.

Definition 3.8 (Corner map). Recall that a *corner* c is an adjacency between a face and a vertex, that we respectively denote $face(c)$ and $vertex(c)$. We define two permutations on the set of corners. If c is a corner, $NaF(c)$ is the next corner around $face(c)$ in clockwise order, while $NaV(c)$ is the next corner around $vertex(c)$ in counter-clockwise order. The inverse permutations are naturally called $PaF(c)$ and $PaV(c)$. A corner is delimited by two edges $NE(c)$ and $PE(c)$: $NE(c)$ joins $vertex(c)$ and $vertex(NaF(c))$ and separates $face(c)$ and $face(NaV(c))$, while $PE(c)$ joins $vertex(c)$ and $vertex(PaF(c))$ and separates $face(c)$ and $face(PaV(c))$.

The *corner map* of a map m is the oriented map whose vertices are the corners of m and which has for any corner c an edge from c to $NaV(c)$ and an edge from c to $NaF(c)$.

Note that the corner map is a bicolored 4-valent graph, endowed with a bicolored orientation. These definitions can be visualized in Fig. 6a.

A formal definition of the opening algorithm, seen as an oriented walk on the corner map, is given in Algorithm 2, and illustrated in Fig. 5.

Algorithm 2 The opening algorithm.

Input: A map m embedded on a surface \mathcal{S} , rooted at a corner c_0 , along with an orientation.

Output: An oriented blossoming embedded graph $b = \text{open}(m)$, embedded on \mathcal{S} .

Set $c = c_0$, $b = \emptyset$, and $E_V = \emptyset$ (E_V is the set of visited edges).

```

repeat
  e = NE(c).
  if e ∉ E_V and e is oriented toward vertex(c) then
    add e to E_V
    add e to b
    c ← NaF(c)
  else if e ∉ E_V and e is outgoing from vertex(c) then
    add e to E_V
    Add a bud to b in place of e.
    c ← NaV(c)
  else if e ∈ E_V and e is oriented toward vertex(c) then
    Add a leaf to b in place of e.
    c ← NaV(c)
  else if e ∈ E_V and e is outgoing from vertex(c) then
    c ← NaF(c)
end if
until c = c_0
return b.
    
```

This alternative definition highlights well the known symmetry between the roles of faces and vertices in the opening algorithm, which we express in Lemma 3.11, and illustrate in Fig. 6b. In addition to Definition 3.2, the following two definitions are needed.

Definition 3.9 (*Reflected map*). To a map m we associate a *reflected map* \tilde{m} which is the same as m except that we switch the orientation of the underlying surface, which amounts to exchanging clockwise and counterclockwise, left and right.

Definition 3.10 (*Complement submap*). To a subgraph s of a graph g we associate the *complement subgraph* s^c defined with the same set of vertices as g along with all edges in g but not in s . This definition is naturally extended to the complement of a map by preserving the embedding.

Lemma 3.11. *Up to a change of orientation of the surface, a map and its dual yield complement interior submaps by the opening algorithm:*

$$\text{Open}(m)^\circ = \left(\left(\text{Open}(\tilde{m}^*)^\circ \right)^* \right)^c,$$

where the complement is taken with respect to m .

The reason why we use the interior map is that duality and complementarity are only defined for non-blossoming map. See Fig. 6b for an illustration of Lemma 3.11.

Proof. Let m be a map, c a corner of m , and c^* its dual corner, in \tilde{m}^* . It is easy to see (cf. Fig. 6a) that $\text{NaF}(c)$ and $\text{NaV}(c^*)$ (resp. $\text{NaV}(c)$ and $\text{NaF}(c^*)$, $\text{PaF}(c)$ and $\text{PaV}(c^*)$, $\text{PaV}(c)$ and $\text{PaF}(c^*)$) are the same corners (in dual maps), and that $\text{NE}(c)$ and $\text{NE}(c^*)$ (resp. $\text{PE}(c)$ and $\text{PE}(c^*)$) are dual edges.

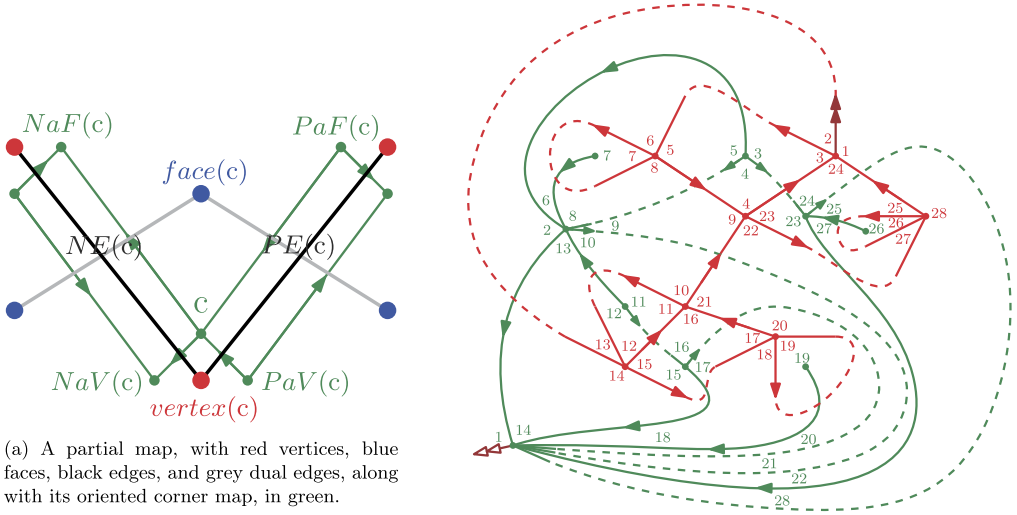


Fig. 6. The opening algorithm is a walk on the corner map.

Let us run Algorithm 2 in parallel on m and \widetilde{m}^* , and show that the order in which dual corners are visited. This is done by induction: suppose that after k steps, the visited corners are exactly dual one from each other, and that the set of visited edges are also dual one from each other. If one algorithm reaches step 1 (resp. step 2), the other reaches step 2 (resp. 4). In any cases they either both add or both don't add e to E_V , and exactly one keeps e as an edge in b , while the other creates a stem instead.

Hence the walks on the dual corner maps are the same, and the resulting dual maps are complement one to another. \square

3.3. Opening a bicolourable map

We are now willing to apply the opening algorithm to bicolourable maps with dual-geodesic orientation, and prove that this yields a bijection. We first describe some properties that will prove useful to describe the resulting maps.

Definition 3.12 (Well-oriented map). A unicellular map b is *well-oriented* if in a tour of the face starting from the root, each edge is first followed backward and then forward.

If b is a tree, this means that any interior edge is oriented toward the root. Note that this definition does not depend on whether the tour is clockwise or counterclockwise.

Any unicellular map has a unique well-orientation, which can be straightforwardly obtained by doing a tour of the face. In relation to Remark 3.3, and in view of Section 4.1,

this implies that the interior orientation of a well-rooted well-oriented unicellular blossoming map b can be easily recovered from the unrooted map \bar{b} if we know which rootable stem of \bar{b} is the root of b .

Definition 3.13 (*Well-labeled map*). A blossoming oriented map is said to be *well-labeled* if its corners are labeled in such a way that:

- the labels of two corners adjacent around a vertex differ by 1, in which case the higher label is to the right of the separating edge (or stem),
- the labels of two corners adjacent along an edge coincide, and
- the root bud has labels 0 and 1.

Looking at the sequence of labels of corners around any fixed vertex, it is clear that the orientation of a well-labeled map is in particular Eulerian. Note that if the map has no stem, then having a well-labeling is equivalent to having a bicolable orientation (indeed, the orientation of a dual edge corresponds to the difference of label between its endpoints, so that any dual cycle has as many forward and backward edges). In particular, this is stronger than having an Eulerian orientation.

The set of well-rooted well-labeled well-oriented unicellular blossoming maps, counted by vertex degrees (similarly to bicolable maps), is denoted \mathcal{O} . The subset of \mathcal{O} made of 4-valent maps is denoted \mathcal{O}^\times .

Recall from Equation (1) that the weight of a bicolable map m is $\prod_{k>0} z_k^{v_{2k}(m)}$. Therefore, two maps have the same weight if and only if they have the same repartition of vertex degrees.

We can now state our main bijective theorem:

Theorem 3.14. *When performed on the dual-geodesic orientation, the opening algorithm is a weight-preserving bijection from \mathcal{BC}_g to \mathcal{O}_g , whose inverse is the closing algorithm. Therefore, $BC_g(\mathbf{z}) = O_g(\mathbf{z})$.*

Applying Theorem 3.14 to $\mathbf{z} = (0, z, 0, \dots)$ and using Proposition 2.10, we obtain the following corollary:

Corollary 3.15. *The opening algorithm on 4-valent bicolable maps yields:*

$$M_g(z) = O_g^\times(z).$$

Remark 3.5. A more complete study of the opening algorithm in higher genus was carried in [6] by Bernardi and Chapuy. Instead of oriented maps, they consider covered maps, that are maps with a marked unicellular spanning submap, and show that they are in correspondence with oriented maps equipped with a so-called *left-connected* orientation. They show that the opening of such oriented maps gives rise to a unicellular spanning submap. However, this submap can be of any genus smaller or equal to the genus of the

underlying surface. We could show that the dual-geodesic orientation is left-connected to conclude that the opening algorithm yields a unicellular spanning submap, but we would still have to prove that this map is of maximal genus. However, in our particular case, because the chosen orientation is not any left-connected orientation, but the dual of the geodesic orientation, we don't need to use this result. We show directly that the opening of a map with geodesic orientation is easily described, and use Lemma 3.11 to conclude about maps with dual-geodesic orientation.

Proof of Theorem 3.14. We first prove that the opening of a map of \mathcal{BC}_g is in \mathcal{O}_g , then that the closure of a map \mathcal{O}_g is in \mathcal{BC}_g , and finally prove that they are inverse bijections.

- Applying the opening algorithm on a bicolored map of genus g endowed with its dual-geodesic orientation yields a well-rooted well-labeled well-oriented unicellular blossoming map of genus g with same weight:

We look at the opening of a bipartite map endowed with its geodesic orientation. A direct analysis of the algorithm implies that, in this case, the blossoming map obtained is the rightmost breadth-first-search exploration tree, along with its buds and leaves.

Now let m be a bicolored map with its dual-geodesic orientation, and o the opening of m . Because of Lemma 3.11, we know that o° is the dual of the complement of the leftmost breadth-first-search exploration tree of m^* starting from the root. In particular, it is a unicellular map of maximum genus.

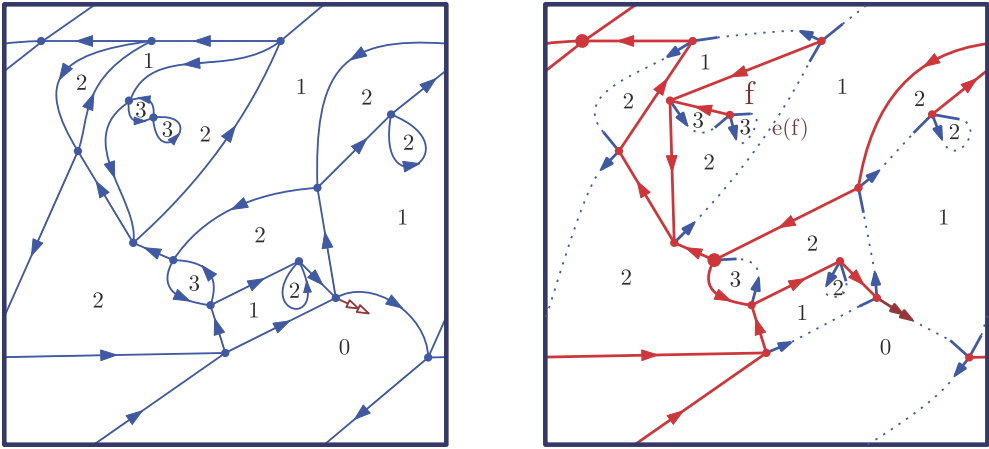
Since the walk on the corner map of m corresponding to the opening algorithm corresponds to a clockwise tour of the unique face of o starting from the root, the rules of the algorithm naturally imply that o is both well-oriented and well-rooted. If we label each corner of o with the distance in m^* from its adjacent face to the root face, then o is also well-labeled.

- The closure of a map $o \in \mathcal{O}_g$ yields a bicolored map m of genus g with same weight and with dual-geodesic orientation:

Let o be a map of \mathcal{O}_g and $m = \text{Close}(o)$. By construction, during the closing algorithm, no stem remains unmatched, and the created edges are non-crossing. This implies that m is indeed correctly embedded, and has genus g (and not more).

Since o is well-labeled, the height in the contour word corresponds to the labels of the corners. By consequence, the labels of corners that become adjacent along an edge by the merge of two stems are the same. Therefore, after the closure, each face of m can be naturally labeled by the common label of its corners.

This labeling on faces corresponds to a labeling of dual vertices such that two adjacent vertices have label that differ by 1 exactly. This implies that the orientation of m^* is a bipartite orientation, and equivalently that the orientation of m is bicolored. Hence, thanks to Corollary 2.19, in order to conclude that m is endowed with its dual-geodesic



(a) A map of \mathcal{BC}_1^x with its dual-geodesic orientation.

(b) A map of \mathcal{O}_1^x .

Fig. 7. A 4-valent bicolorable map with dual-geodesic orientation, and its opening.

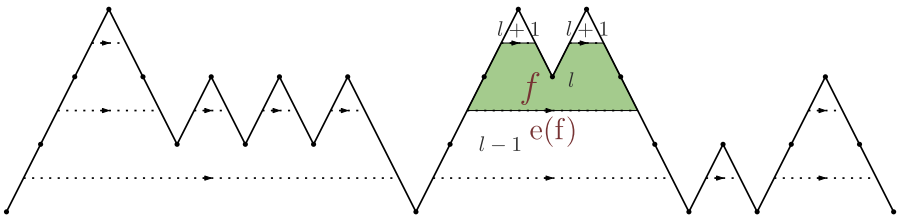


Fig. 8. The contour word of the map displayed in Fig. 7b. The face f , after closure, has 1 counterclockwise adjacent edge, called $e(f)$.

orientation, we just have to prove that the map m has no clockwise face other than the root face.

A non-root face f of m with label l is enclosed by a certain number (possibly 0) of edges of o , a certain number (possibly 0) of edges formed by merging a bud and a leaf with adjacent labels l and $l + 1$, and exactly one edge formed by merging a bud and a leaf with adjacent labels $l - 1$ and l (see Fig. 8 for an example). This last edge is denoted $e(f)$.

By definition, $e(f)$ is formed by the merging of a bud and a leaf, coming in this order in a clockwise tour of the face starting from the root. By consequence, f is on the left of $e(f)$, which implies that f is not clockwise.

- The two operations are inverse bijections:

Applying the opening algorithm to the closure of a well-rooted well-labeled well-oriented unicellular blossoming map b yields the original map b itself. Indeed, any closure edge is first met outgoing (see Remark 3.1 on well-rooted maps), whereas any non-closure edge is first met ingoing, because b is well-oriented.

\mathcal{M}_g	Maps of genus g	
BC_g^\times	4-valent bicolored maps of genus g	Proposition 2.10: $M_g(z) = BC_g^\times(z)$
\mathcal{O}_g^\times	well-rooted well-labeled well-oriented blossoming unicellular maps of genus g	Corollary 3.15: $M_g(z) = O_g^\times(z)$
\mathcal{U}_g	well-labeled well-oriented blossoming unicellular maps of genus g	Theorem 4.1: $O_g^\times(z) = z^{2g-1} \cdot \frac{2}{z} \int_0^z U_g(t) dt$
\mathcal{T}	rooted binary trees oriented toward the root, with 2 buds on each inner vertex	Decomposition: $T(z) = z + 3T(z)^2$
\mathcal{P}_g	pruned well-labeled well-oriented blossoming unicellular maps of genus g	Lemma 4.6: $U_g(z) = \frac{\partial T}{\partial z} \cdot P_g(T(z))$
\mathcal{R}_g	scheme-rooted pruned well-labeled well-oriented blossoming unicellular maps of genus g	Lemma 4.8: $P_g(z) \simeq \frac{1}{2g-v_4^g} \cdot \frac{\partial(tR_g(t))}{\partial t}(z)$

Fig. 9. A recap of some families of maps, and some relations between them.

Reciprocally, if the opening of an oriented map m of genus g yields a unicellular blossoming map b of genus g , then the closure of b yields m . Indeed, there is a unique way to do a planar matching of the stems of b . \square

4. Enumeration and rationality

Although the opening bijection works for any bicolored map, we now restrict our work to 4-valent bicolored maps, keeping in mind that these are in bijection with general maps. The next two sections develop the analysis of the family \mathcal{O}_g^\times , so as to obtain a bijective proof of Theorem 1.1, through Corollary 3.15.

Fig. 9 gives a recap of the definitions and relations between some sets of maps, that have already been defined or will be in the upcoming section. It can be used as an outline of our work up to Section 4.3.

4.1. Getting rid of well-rootedness

The analysis of objects such as the maps of \mathcal{O}_g^\times is made difficult by the non-locality of a condition such as well-rootedness. The following theorem enables to go past that condition in the rest of the analysis.

The generating series of \mathcal{O}_g^\times where maps are counted by leaves instead of vertices is denoted ${}^lO_g^\times$. A straight-forward calculation from Euler’s formula gives $O_g^\times(z) = z^{2g-1} \cdot {}^lO_g^\times$. The set of rooted (but not necessarily well-rooted) well-labeled well-oriented 4-valent unicellular maps, counted by leaves, is denoted \mathcal{U} . Recall Definition 3.7 for the definition of the unrooted map.

Theorem 4.1. *Let \overline{m} be an unrooted map with $n + 1$ rootable stems (which means its representants, the corresponding rooted maps, have n leaves and n buds).*

There is a 2-to- $(n + 1)$ application from rooted well-labeled well-oriented 4-valent unicellular map with unrooted map \overline{m} , to well-rooted well-labeled well-oriented 4-valent unicellular map with unrooted map \overline{m} .

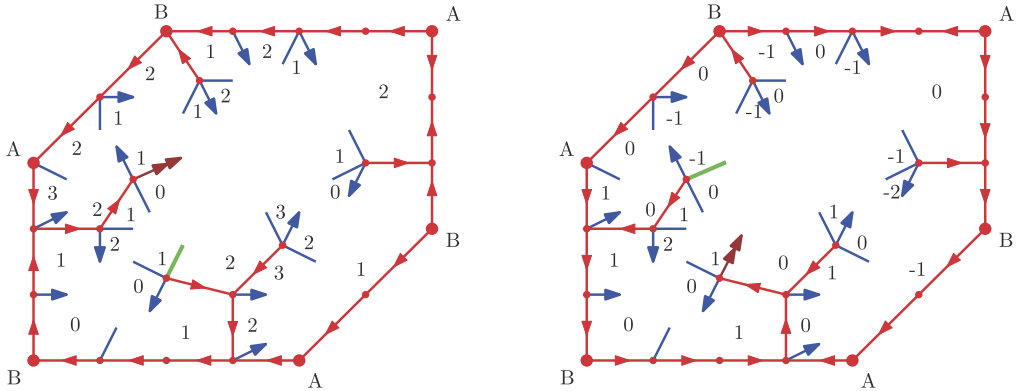


Fig. 10. A map of \mathcal{O} with a marked rootable stem (in green) is bijectively mapped (by the rerooting algorithm) to a map of \mathcal{U} with a marked well-rootable stem (in green). In the 2 maps the opposite sides are identified, so that the maps are of genus 1, and the 2 scheme vertices are A and B.

Recall the definition of a well-rootable stem, given in Definition 3.6. Theorem 4.1 directly follows from Lemma 4.2:

Lemma 4.2. *There is a bijection, called rerooting, between rooted well-labeled well-oriented 4-valent unicellular maps with unrooted map \overline{m} , $2n$ stems and a marked well-rootable stem, and well-rooted well-labeled well-oriented 4-valent unicellular maps with unrooted map \overline{m} , $2n$ stems and a marked rootable stem.*

Lemma 4.2 is illustrated in Fig. 10.

Proof. Let o be a well-rooted well-labeled well-oriented 4-valent unicellular map with unrooted map \overline{m} , $2n$ stems and a marked rootable stem.

The *rerooting* algorithm is defined as follows: if the marked stem is the root, we do nothing at all. Otherwise, the root bud and the marked leaf are joined into a single oriented edge. This divides the face into 2 faces called: f_L and f_R , on the left and right of the newly created edge. We decrease all labels of corners of the sub-face f_L by 2. The orientation of the new edge is reversed, and it is then cut back into a bud and a leaf. The former root is marked, and the former marked leaf becomes the root bud. The interior orientation is then redefined so that the map is well-oriented, which can be easily done by doing a tour of the face.

The rerooted map is denoted u . It is by definition a rooted well-oriented 4-valent unicellular map with unrooted map \overline{m} , $2n$ stems and a marked rootable stem. The contour word of u is obtained from that of o by a cyclic permutation, and by consequence, since o is well-rooted, the marked edge of u is well-rootable.

In order for the obtained labeling and orientation to fulfill the last condition of a well-labeled map (recall Definition 3.13), in case the root does not already have labels 01, all labels will be shifted accordingly in the end. However this does not alter the

first 2 conditions, and we therefore proceed to prove, before shifting, that they are satisfied.

Two labels adjacent along an edge were either both unchanged, or both reduced by 2. Two labels separated by a stem which is not marked nor the root are unchanged. Out of the two labels separated by a marked stem or the root, one is unchanged, and the other is reduced by 2. However the orientation of the stem is also changed. In all these cases, the labels remain compatible with the orientation after rerooting.

Claim 4.3. *An interior edge has opposite orientation before and after rerooting if and only if it separates f_L and f_R , in which case, before rerooting, f_L is on its right and f_R on its left.*

Proof. Because we deal with well-oriented maps, the orientation of the interior edges in the map before and after rerooting are determined by the order of apparition of their sides in a tour of the face starting from the root.

If both sides of the edge are adjacent to the same sub-face, they appear in the same order in a clockwise tour of the face starting from the root before and after rerooting, which implies that the orientation of the edge is unchanged by the rerooting.

If the two sides of the edge are not adjacent to the same sub-face, then the well-orientedness of the map before and after rerooting implies that the edge is counter-clockwise around f_L and clockwise around f_R before rerooting, whereas it is clockwise around f_L and counter-clockwise around f_R after rerooting. \square

Now we consider two adjacent corners separated by an edge e , and check that their labels are compatible with the orientation of e .

If the two sides of e are both adjacent to f_R , the labels and orientation were unchanged, so they remain compatible. If the two sides of e are both adjacent to f_L , the orientation was unchanged whereas the label were both reduced by 2, so they remain compatible.

If e has one side on each sub-face, then before rerooting, the label in f_L was higher than the other one by 1, whereas after rerooting it is reduced by 2, and is hence smaller than the other (unchanged) label by 1. Since both o and u are well-oriented, this is compatible with the change of orientation of the edge.

A very similar proof can be made for the inverse bijection. \square

The considered families of maps can be restricted by unrooted map, so that for instance ${}^l\mathcal{O}_{\overline{m}}^\times$ is the subset of ${}^l\mathcal{O}$ whose unrooted map is the 4-valent unrooted map \overline{m} .

Corollary 4.4. *The following holds:*

$${}^l\mathcal{O}_{\overline{m}}^\times(t) = \frac{2}{t} \int_0^t U_{\overline{m}}(z) dz.$$

Proof. The bijection of Theorem 4.1 yields: $(n + 1) \cdot [t^n]O_{\overline{m}}^{\times}(t) = 2 \cdot [t^n]U_{\overline{m}}(t)$, which leads to the equation on generating functions. \square

4.2. Reducing a unicellular map to a labeled scheme

The framework applied in this subsection has become classical when studying unicellular maps. In particular, it is developed by Chapuy, Marcus and Schaeffer in [16].

Definition 4.5 (*Extended scheme*). The *extended scheme* of a unicellular blossoming map u is the unicellular map of genus g obtained by iteratively removing from the interior map u° all vertices of interior degree 1.

A unicellular map u is composed of an extended scheme upon which are attached some stems and treelike parts. These treelike parts, with their leaves, are binary trees, oriented towards the root of the map. Furthermore, on each interior vertex of these trees is attached a bud. The set of such trees, counted by leaves, is denoted \mathcal{T} . Its generating series satisfies the recurrence relation $T(z) = z + 3T(z)^2$. The generating series of such trees with a marked leaf (or equivalently doubly rooted) is $z \cdot \frac{\partial T}{\partial z}(z)$.

The *pruning* procedure is defined as follows: each treelike part is replaced by a rootable stem: a root bud if the tree contains the root, a leaf otherwise (see Fig. 11 left and middle). The image of \mathcal{U} by the pruning procedure, counted by leaves, is denoted \mathcal{P} .

Lemma 4.6. *The pruning algorithm yields:*

$$U(z) = \frac{\partial T}{\partial z} \cdot P(T(z)).$$

Proof. In order to recover a map of \mathcal{U} from a pruned map p , we need to replace each leaf of p by a tree. Then the root bud of p (which has weight 0) is replaced by a tree with a marked leaf. The marked leaf is replaced by a root bud (decreasing the weight by 1), and the tree is oriented toward this new root. The equation follows. \square

All vertices of the pruned map are of interior degree 2, 3 or 4. We call v_2^s , v_3^s , and v_4^s the number of such vertices. When the notation is ambiguous, we specify which map is concerned by writing $v_2^s(m)$ for example. A quick calculation based on Euler formula gives: $v_3^s + 2v_4^s = 4g - 2$. There are thus a bounded number of vertices of degree 3 or 4, the other ones being of degree 2. Vertices of interior degree at least 3 in the pruned map are called *scheme vertices*, and a stem (resp. bud, leaf) attached on a scheme vertex (which is then necessarily of interior degree 3 since the map is 4-valent) is called a *scheme stem* (resp. *scheme bud*, *scheme leaf*). A map is said to be *scheme-rooted* if its root is a scheme bud. After pruning, a sequence of adjacent vertices (of interior degree 2) between two scheme vertices is called a *branch*.

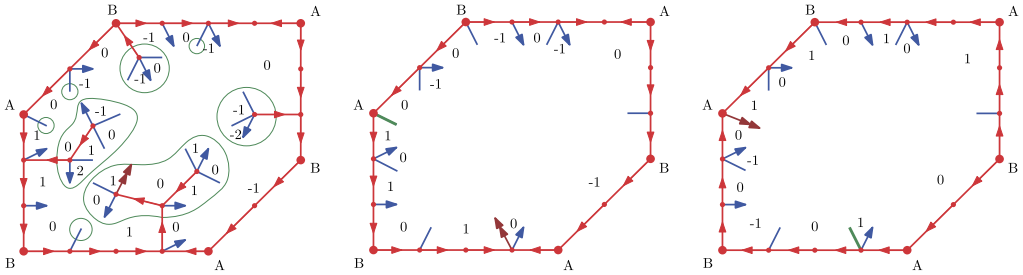


Fig. 11. On these maps, the three pairs of opposite sides are identified, so that they only have 2 scheme vertices each, denoted A and B . A map of \mathcal{U} (left), whose treelike parts are encompassed in green, is pruned (middle). One of its scheme rootable stems is marked (in green), and the map is then rerooted (right) on this marked stem, while marking (in green) the former root stem.

Lemma 4.7. *Let $p \in \mathcal{P}$. Out of its $v_3^s = 4g - 2v_4^s - 2$ scheme stems, p has exactly $2g - v_4^s$ rootable scheme stems. In particular $v_3^s > 0$.*

Proof. • Suppose the map p is scheme-rooted. Since p is well-oriented, all edges of a branch are oriented the same way, which implies that all vertices of interior degree 2 have interior out- and in-degree equal to 1.

By consequence, the sums of interior in- and out-degrees of scheme vertices are equal. Since the map is Eulerian, the sum of blossoming in- and out-degrees of scheme vertices are equal. Hence there are as many scheme buds as scheme leaves, that is $2g - v_4^s - 1$ each.

- Conversely, if the root is on a vertex of interior degree 2, the root-vertex has interior in-degree 2 and interior out-degree 0, whereas all other vertices of interior degree 2 have interior out- and in-degree equal to 1.

By consequence, the sum of interior out-degrees of scheme vertices is equal to the sum of interior in-degrees of scheme vertices, plus 2. Since the map is Eulerian, the sum of blossoming in-degrees of scheme vertices is equal to the sum of blossoming out-degrees of scheme vertices, plus 2. Hence there are $2g - v_4^s$ scheme leaves and $2g - v_4^s - 2$ scheme buds.

In any case there is a positive number of scheme stems, which implies that $v_3^s > 0$. □

We now proceed to reroot the pruned map on a scheme stem. We choose a rootable scheme stem among the $2g - v_4^s$ possible choices and mark it. The *rerooting-on-the-scheme* algorithm (see Fig. 11 middle and right), is the same as the rerooting described in the proof of Lemma 4.2.

The subset of \mathcal{P} composed of *scheme-rooted* maps is denoted \mathcal{R} . We call $\mathcal{P}^{\bar{e}}$ (resp. $\mathcal{R}^{\bar{e}}$) the subset of maps of \mathcal{P} (resp. \mathcal{R}) that have \bar{e} as an unrooted extended scheme.

Lemma 4.8. *The rerooting-on-the-scheme algorithm yields:*

$$P_{\bar{e}}(z) = \frac{1}{2g - v_4^s(\bar{e})} \cdot \frac{\partial(tR_{\bar{e}}(t))}{\partial t}(z).$$

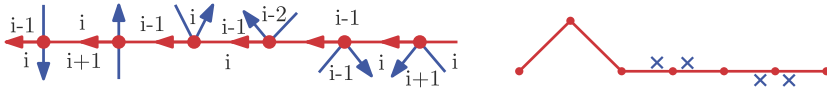


Fig. 12. An example of a branch displaying the 6 possible types of vertices of degree 2, and the corresponding weighted Motzkin path.

Now that the map is rooted on a scheme bud, since it is well-oriented, all edges of a branch have the same orientation. We call *merging* the procedure that replaces each branch by a single edge with the same orientation (see Fig. 13).

The map we obtain is called the *labeled scheme*. It is not well-labeled because corners adjacent along an edge do not necessarily have the same label anymore, but the rule around a vertex is still respected. The set of labeled schemes is denoted \mathcal{L} .

4.3. Analyzing a scheme

For $l \in \mathcal{L}$, we now want to determine which maps have l as labeled scheme. Each edge of l should be replaced by a valid branch. However we need to be sure that after replacement, the map is well-labeled, and agrees with the labeling of the scheme. Therefore, following [16], we express the generating series of branches with prescribed height on the extremities.

There are 6 types of vertices of interior degree 2, displayed in Fig. 12 left. If the bud and leaf are on opposite sides, the label of the corners either increases on both side or decreases on both sides. In the 4 other cases, the stems are on the same side, and the label remains the same before and after the vertex. Therefore each type of vertex of interior degree 2 can be represented by a step, depending on the variation of the labels around it: an up-step if the label increases, a down-step if it decreases, and 4 types of horizontal steps if it stays the same, represented with a blue cross placed accordingly to the position of the bud (see Fig. 12 right). These steps are called *weighted Motzkin steps*, and together they form a *weighted Motzkin path*, whose variation of height corresponds to the variation of labels of the corresponding branch.

An edge of the labeled scheme going from label i to label j can therefore be replaced by a weighted Motzkin path going from height i to height j , as illustrated in Fig. 13.

We denote by \mathcal{D} the set of weighted Motzkin paths going from height 0 to height -1 , that remain non-negative before the last step, counted by length, and by \mathcal{B} the set of weighted Motzkin paths going from height 0 to height 0, counted by length. Following [22, p. 76–77], we obtain the following decomposition equations:

$$D = z(1 + 4D + D^2)$$

$$B = 1 + 4zB + 2zDB.$$

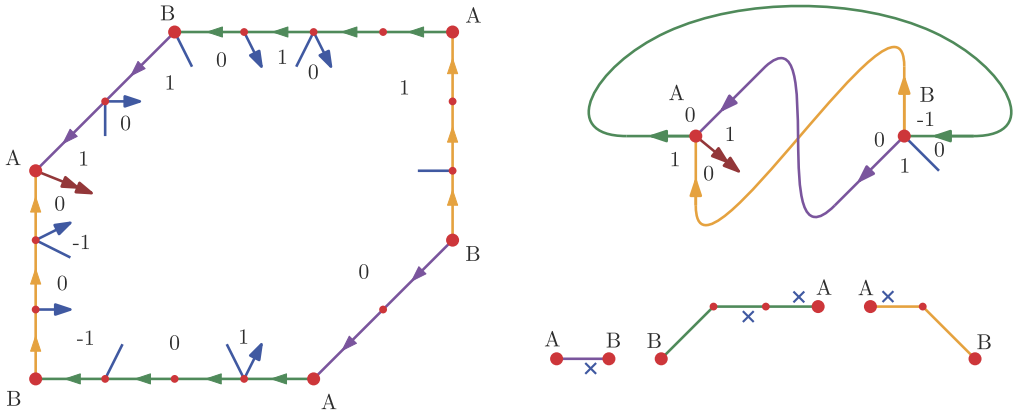


Fig. 13. Reducing a map of \mathcal{R} to a labeled scheme, by replacing each branch by a weighted Motzkin path.

After combination of the two equations, B is rewritten as a function of D only:

$$B = \frac{1 + 4D + D^2}{1 - D^2}.$$

The generating series of paths going from height i to j is: $B \cdot D^{|i-j|}$.

Remark 4.1. The role of B and D is very similar to the role of B and U in the work of Chapuy, Marcus and Schaeffer in [16]. A few subtle differences may be noted: in our case there are 4 different horizontal steps instead of only 1. Furthermore, an element of \mathcal{B} may be of length 0, which is not the case in [16], and leads to simpler formulae.

Recall that our purpose is to prove that $M_g(t)$, the series of maps of genus g , is rational in t . Using the lemmas of Section 4, we will be able to express the generating series in terms of the auxiliary function D . A key observation of [16] is that rationality in t amounts to symmetry in D , thanks to Lemma 4.9.

For a function Ψ in D , we denote its *transposition* $\overline{\Psi}(D) = \Psi(D^{-1})$. We say that Ψ is *symmetric* (resp. *antisymmetric*) in D if $\Psi = \overline{\Psi}$ (resp. $\Psi = -\overline{\Psi}$). Note for example that B is antisymmetric.

Lemma 4.9. *A function is rational in z if and only if it is rational and symmetric in D .*

Proof. Since $z = \frac{1}{D^{-1}+4+D}$, any function which is rational in z is rational and symmetric in D .

Let f be a function rational and symmetric in D , whose irreducible expression is $\frac{P}{Q}$. We denote d the average degree of P , which is half the sum of the higher and lower degree of P . By symmetry, it is also the average degree of Q . By symmetry, $P \cdot D^{-d}$ and $Q \cdot D^{-d}$ are both symmetric in D and D^{-1} . In case d is not an integer, $P \cdot D^{-d}$ and

$Q \cdot D^{-d}$ are not polynomials in D and D^{-1} . However, in this case, $P \cdot D^{-d} \cdot (D^{-\frac{1}{2}} + D^{\frac{1}{2}})$ and $Q \cdot D^{-d} \cdot (D^{-\frac{1}{2}} + D^{\frac{1}{2}})$ are symmetric polynomials in D and D^{-1} .

Therefore, in any case, f can be written as the ratio of 2 symmetric polynomials. Since the family of polynomials $z^{-k} = (D^{-1} + 4 + D)^k$ generates all symmetric polynomials, f can be written as a rational function of z^{-1} , which is enough to conclude the proof. \square

Definition 4.10 (*Unlabeled scheme*). An *unlabeled scheme* is a scheme where we forgot all labels. We denote by \mathcal{S} the set of unlabeled schemes. The set of unrooted unlabeled scheme is denoted $\overline{\mathcal{S}}$.

We specialize our classes of maps depending on the scheme obtained by following the previous steps. For instance, \mathcal{R}_s is the set of maps $r \in \mathcal{R}$ whose scheme is s .

Similarly, $\mathcal{M}_{\overline{s}}$ is the set of maps such that, if you apply the radial construction, then the opening algorithm, then the first rerooting, then the pruning, then the second rerooting, then replace branches by edges, then forget labels (see Fig. 9), you obtain a scheme whose unrooted version is \overline{s} .

Remark 4.2. The family \mathcal{M} will be restricted by unrooted scheme rather than unlabeled scheme. Indeed, the rerooting procedures are many-to-many applications rather than bijections, which means that going through them does not associate a fixed unlabeled scheme to a given map. Rather, it associates several unlabeled schemes, that all have the same unrooted scheme.

We denote R^b the generating series of \mathcal{R} , counted only by leaves attached on a branch, instead of all leaves, and R_s^b its restriction to maps with unlabeled scheme s . Note that $R_s(z) = z^{2g - v_4^s(s) - 1} R_s^b(z)$.

Theorem 4.11. For any $s \in \mathcal{S}$, R_s^b is rational and symmetric in D .

Section 5 will be dedicated to prove Theorem 4.11. To that end, an additional study on the structure of the schemes will be required, that will be carried on in Section 4.4.

In the rest of Section 4.3, we show that Theorem 4.11, in conjunction with the work of Section 4, leads to Theorem 4.12, a refined version of Theorem 1.1, where the unrooted scheme obtained by our bijection is specified.

Theorem 4.12. For any \overline{s} in $\overline{\mathcal{S}}$, the generating series $M_{\overline{s}}(t)$ is a rational function of $T(t)$.

Since $\overline{\mathcal{S}}_g$ is finite for any fixed g , this theorem implies that $M_g(t) = \sum_{\overline{s} \in \overline{\mathcal{S}}_g} M_{\overline{s}}(t)$ is rational in $T(t)$, which is equivalent to Theorem 1.1.

Remark 4.3. The main reason why we are able to obtain the rationality of M_g is that, unlike in [16], the rationality holds for each scheme, which makes it possible to analyze

more specifically one scheme at a time. The reason why maps are rational by scheme in our case but not in [16] remains somewhat of a mystery.

Proof of Theorem 4.12. We derive from the previous sections (see also Fig. 9) that:

$$\begin{aligned}
 M_{\bar{s}}(t) &= BC_{\bar{s}}^{\times}(t) \\
 &= O_{\bar{s}}^{\times}(t), && \text{because of Corollary 3.15} \\
 &= t^{2g-1} \cdot {}^l O_{\bar{s}}(t), && \text{by definition} \\
 &= t^{2g-1} \cdot \frac{2}{t} \int_0^t U_{\bar{s}}(z) dz, && \text{because of Corollary 4.4} \\
 &= 2t^{2g-2} \int_0^t \frac{dT}{dz} \cdot P_{\bar{s}}(T(z)) \cdot dz, && \text{because of Lemma 4.6} \\
 &= \frac{2t^{2g-2}}{2g - v_4^s(s)} \int_0^t \frac{d(uR_{\bar{s}}(u))}{du}(T(z)) \cdot \frac{dT}{dz} \cdot dz, && \text{because of Lemma 4.8} \\
 &= \frac{2t^{2g-2}}{2g - v_4^s(s)} \cdot T(t) \cdot R_{\bar{s}}(T(t)), && \text{by a change of variable}
 \end{aligned}$$

Hence, in order to prove that $M_{\bar{s}}(t)$ is rational in T (and t), it suffices to prove that $R_{\bar{s}}(z)$ is rational in z , or equivalently that $R_{\bar{s}}$ is rational and symmetric in D , thanks to Lemma 4.9. For all $\bar{s} \in \bar{\mathcal{S}}$, we have $R_{\bar{s}} = \sum_{\substack{t \in \mathcal{S} \\ \bar{t} = \bar{s}}} R_t$.

Therefore, Theorem 4.11 is enough to conclude the proof. \square

Remark 4.4. Note that we apply twice the rerooting algorithm, the first time from a well-rootable stem to any rootable stem, and the second time from a rootable stem to a rootable scheme stem. In the course of the proof of Theorem 4.12, these two operations, in terms of generating functions, correspond to an integral and a derivative. Although the two rerooting operations are separated by the pruning operation, it appears that a change of variable allows the integral and derivative to cancel out. This can actually be seen in a combinatorial way, by merging the two rerooting operations and the pruning operation into a single operation, which result in Lemma 4.13.

Lemma 4.13. For any unrooted scheme \bar{s} , there is a $(2g - v_4^s(\bar{s}))$ -to-2 application from maps of $\mathcal{O}_{\bar{s}}^{\times}$ to maps of $\mathcal{R}_{\bar{s}}$ with a tree associated to each of its rootable stems.

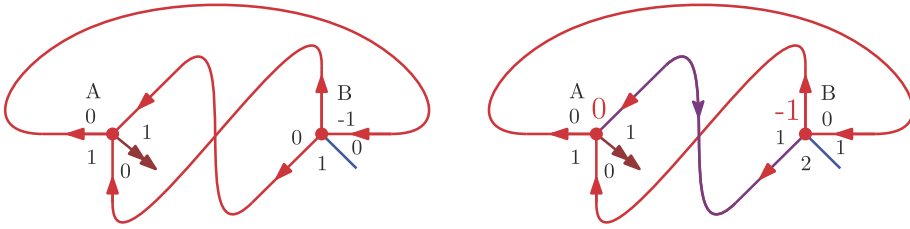


Fig. 14. The scheme on the left has the usual labels. On the right, these labels define labels on vertices (red), and offset labels (black). An offset oriented edge (purple) appears. Here, the offset graph is reduced to this single offset edge.

4.4. The offset graph

We now label each scheme vertex with the minimal label of its corners, and relabel the corners relatively to this minimum, by subtracting the vertex label from each corner label. This second label is called the *offset label*. In case the outgoing and ingoing edges around a vertex are alternated, the offset labels around the vertex are 0101. Otherwise, the sequence is 0121.

The edges of the scheme can be of two different types. Look at the offset labels around it. If the offset labels are the same (01 or 12) on both sides, the edge is called *level*. If the labels are 01 on one side and 12 on the other, the edge is *offset* toward the second one. We define the *offset graph* as the oriented sub-graph of the scheme where only the offset edges are kept, along with their orientation. See Fig. 14 for an example.

Proposition 4.14. *The offset graph of a scheme is acyclic.*

Proof. Let's assume by contradiction that there exists a labeled scheme $l \in \mathcal{L}$ whose offset graph is not acyclic and let C be a simple cycle of the offset graph of l . Since an offset edge ends with relative labels 12, any vertex of type 0101 has indegree 0 in the offset graph, so that all vertices of C are of type 0121.

Let e_1 be the first edge of C visited during a clockwise tour of l starting from the root. Since l is well-oriented, e_1 is visited backward first. Depending on whether it is visited forward or backward in the offset graph, we are in one of the two cases depicted in Fig. 15.

- Assume we are in the leftmost case. Consider now the first visited edge (or stem) adjacent to vertex A , and call it $e_f(A)$. It may be the root bud or a normal edge, but in both cases, $e_f(A)$ has to be visited backward first in the tour, and hence it is either e_3 or e_4 .

Suppose $e_f(A) = e_4$, then e_3 cannot be an interior edge because it would have to be visited backward first in the tour, whereas it is outgoing from A and cannot have been visited before e_4 by definition of $e_f(A)$. Hence e_3 is a bud, and e_2 is visited before e_1 in the tour. If $e_f(A) = e_3$, then e_2 is visited before e_1 .

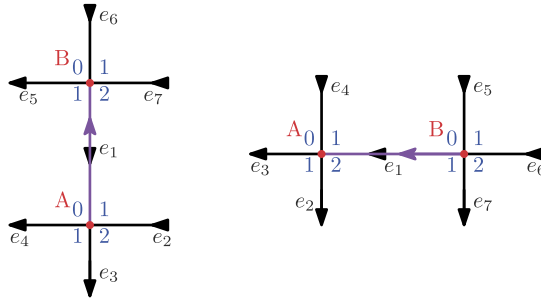


Fig. 15. illustration of the two possible cases of first visited edge of an offset cycle. In both cases, e_2 to e_7 can *a priori* be either stems or edges, and belong or not to the offset graph.

In any case both e_2 and e_3 are visited before e_1 , which implies they are not part of C . This is a contradiction because C is a cycle which is oriented in the offset graph, which means it does not contain e_4 , because e_4 has offset label 01 around A .

- Now assume we are in the rightmost case. We define similarly $e_f(B)$ to be the first visited edge (or stem) around B . Again, since it has to be outgoing, it is either e_1 or e_7 .

Suppose $e_f(B) = e_7$. Then both e_7 and e_6 are visited before e_1 in the tour, which implies they are not in C . Moreover, since e_5 has relative label 01 around B , it cannot be part of the offset cycle C . This is a contradiction.

Therefore $e_f(B) = e_1$. Then similarly to the leftmost case, we conclude that e_7 is a bud. By consequence, since C is a cycle in the offset graph, the edge coming right after e_1 in C has to be e_6 , which has relative label 12 around B .

The same reasoning (we already know we are in the rightmost case) can be applied on e_6 , the second visited vertex of C , and so on. By induction we conclude that C is only made of edges whose orientation in the map and the offset graph coincide. Additionally, the only edges or stems outgoing from C are on its left, whereas the only edges or stems ingoing from C are on its right. We also know that the left part of C is visited backward all at once, from e_1 to e_3 .

Now, in a clockwise tour of the face, which edge (or stem) $e_f^r(C)$ is visited just before the first time we meet the right side of C ? Since in the tour, $e_f^r(C)$ has to be visited backward first (even if it is the root), it can not be any of the edges or stems on the right of C . Since there is no good candidate for $e_f^r(C)$, there is a contradiction, which implies that the offset graph is acyclic. \square

5. Rationality of maps with a given scheme

In this section we prove Theorem 4.11. Throughout all the section, s is an unlabeled scheme.

5.1. Counting rerooted pruned maps

We now proceed to compute the generating function of all maps with a fixed unlabeled scheme. A branch from height i to height j in a scheme contributes for $B \cdot D^{|i-j|}$. To get the total participation of an unlabeled scheme to R_s^b , we need to sum over all possible labelings of the vertices. To deal with the relativity of label, instead of requiring that the root has label 01, we arbitrarily decide that the lowest height has to be 0, which is not equivalent since the maps are not necessarily well-rooted.

To make things simpler, we first analyze the case of an unlabeled scheme s with no offset edge. In this case, we obtain:

$$R_s^b = \sum_{\substack{h_1 \cdots h_{n_v} \in \mathbb{N} \\ \min(h_1, \dots, h_{n_v}) = 0}} \prod_{\substack{(v_i, v_j) \in \mathcal{E}(s) \\ i < j}} B \cdot D^{|h_i - h_j|}.$$

For a given affectation of heights, we define a function characterizing the ordering of heights of vertices. We set k to be the total number of distinct heights. To each vertex v_i we associate an integer $o(i)$ between 1 and k such that $h_i < h_j$ (resp. $h_i = h_j$, $h_i > h_j$) if and only if $o(i) < o(j)$ (resp. $o(i) = o(j)$, $o(i) > o(j)$). Note that o is necessarily a surjection. The size of the image of a surjection o is denoted $k(o)$. Whenever it is unambiguous, we simply write k . We denote $[n] = \{1, 2, \dots, n\}$. We denote $S(n)$ the set of surjection from $[n]$ to $[k]$, for any k in $[n]$.

We can therefore rewrite the formula for the generating series:

$$R_s^b = B^{n_e} \cdot \sum_{o \in S(n_v)} \sum_{0 = h_1 < \dots < h_k} \prod_{\substack{(v_i, v_j) \in \mathcal{E}(s) \\ i < j}} D^{|h_{o(i)} - h_{o(j)}|}.$$

Remark 5.1. This idea of grouping the labeled schemes that have the same relative ordering of scheme vertices is reminiscent to the use of *standard schemes* in [16].

For a subset S of vertices, we define the cut of a subgraph as: $C(S) = |\{(u, v) \in \mathcal{E}(s) \text{ such that } u \in S \text{ and } v \notin S\}|$. We also define: $\Phi_o(i) = \frac{D^{C(o^{-1}(\{i\}))}}{1 - D^{C(o^{-1}(\{i\}))}}$.

Lemma 5.1. For an unlabeled scheme $s \in \mathcal{S}$ with no offset edge, we have:

$$R_s^b = B^{n_e} \cdot \sum_{o \in S(n_v)} \prod_{i=1}^{k-1} \Phi_o(i).$$

Proof. We apply the change of variables: $I_i = h_{i+1} - h_i$:

$$R_s^b = B^{n_e} \cdot \sum_{o \in S(n_v)} \sum_{I_1, \dots, I_{k-1} \in \mathbb{N}^*} \prod_{\substack{(v_i, v_j) \in \mathcal{E}(s) \\ o(i) \leq o(j)}} D^{I_{o(i)} + I_{o(i)+1} + \dots + I_{o(j)-1}}.$$

Our expression can then be rewritten in terms of cut:

$$\begin{aligned}
 R_s^b &= B^{n_e} \cdot \sum_{o \in S(n_v)} \sum_{I_1, \dots, I_{k-1} \in \mathbb{N}^*} \prod_{i=1}^{k-1} D^{I_i \cdot C(o^{-1}([i]))} \\
 &= B^{n_e} \cdot \sum_{o \in S(n_v)} \prod_{i=1}^{k-1} \sum_{I_i \in \mathbb{N}^*} D^{I_i \cdot C(o^{-1}([i]))} \\
 &= B^{n_e} \cdot \sum_{o \in S(n_v)} \prod_{i=1}^{k-1} \frac{D^{C(o^{-1}([i]))}}{1 - D^{C(o^{-1}([i]))}}. \quad \square
 \end{aligned}$$

Now we take offset edges into account. Since the offset graph is acyclic (Proposition 4.14), we relabel the vertices so that for all oriented offset edge (v_i, v_j) with $i < j$, the edge is offset toward j . In other words, vertices are relabeled according to a linear extension of the partial order induced by the offset graph.

Consider an offset edge $e = (v_i, v_j) \in \mathcal{O}$ with $i < j$. We say that e is a *tie* (resp. an *inversion*, resp. an *anti-inversion*) if $o(i) = o(j)$ (resp. $o(i) > o(j)$, resp. $o(i) < o(j)$). We call n_t (resp. n_i , resp. n_a) the number of ties (resp. inversions, resp. anti-inversions). Whenever it is necessary, we specify which surjection is concerned by writing $n_t(o)$ for instance.

Lemma 5.2. *For any unlabeled scheme $s \in \mathcal{S}$, we have:*

$$R_s^b = B^{n_e} \cdot \sum_{o \in S(n_v)} \left(\prod_{i=1}^{k-1} \Phi_o(i) \right) \cdot D^{n_t(o) + n_a(o) - n_i(o)}.$$

Proof. Consider the formula given in Lemma 5.1. To take offset edges into account, we need to change slightly the weight of each offset edge e . If e is a tie, the corresponding branch was given weight B instead of $B \cdot D$. If e is an inversion, the corresponding branch was given weight $B \cdot D^{h_{o(i)} - h_{o(j)}}$ instead of $B \cdot D^{h_{o(i)} - h_{o(j)} - 1}$. If e is an anti-inversion, the corresponding branch was given weight $B \cdot D^{h_{o(j)} - h_{o(i)}}$ instead of $B \cdot D^{h_{o(j)} + 1 - h_{o(i)}}$. To take these defects into account we therefore need to multiply by a factor depending on the number of inversions, ties, and anti-inversions. This leads to Lemma 5.2. \square

5.2. Proof of Theorem 4.11

We start from the formula of Lemma 5.2 and use the fact that $\overline{\Phi_o(i)} = -(1 + \Phi_o(i))$. Recall that B is asymmetric. Therefore,

$$\begin{aligned} \overline{R}_s^b &= \overline{B}^{n_e} \cdot \sum_{o \in S(n_v)} \left(\prod_{i=1}^{k-1} \overline{\Phi_o(i)} \right) \cdot D^{-n_t - n_a + n_i} \\ &= (-1)^{n_e} \cdot B^{n_e} \cdot \sum_{o \in S(n_v)} \left((-1)^{k-1} \cdot \prod_{i=1}^{k-1} (1 + \Phi_o(i)) \right) \cdot D^{-n_t - n_a + n_i}. \end{aligned}$$

Given two surjections o and p , we say that o *refines* p and p *coarsens* o , and write $o \preceq p$, if:

$$\forall x, y; \quad o(x) = o(y) \Rightarrow p(x) = p(y).$$

This means equivalently that the partial order on vertices induced by o is an extension of the one induced by p .

A term of the development of the product $\prod_{i=1}^{k(o)-1} (1 + \Phi_o(i))$ corresponds to a permutation p that coarsens o ; indeed, for each i , we have to choose 1 or $\Phi_o(i)$ in the product, which corresponds to choosing whether or not to merge $o^{-1}(i)$ and $o^{-1}(i+1)$. Therefore, $\prod_{i=1}^{k(o)-1} (1 + \Phi_o(i)) = \sum_{p \succeq o} \prod_{i=1}^{k(p)-1} \Phi_p(i)$.

Hence we can rewrite the previous expression by first developing the product, and then interverting the two summations:

$$\begin{aligned} \overline{R}_s^b &= (-1)^{n_e} \cdot B^{n_e} \cdot \sum_{o \in S(n_v)} \left((-1)^{k(o)-1} \cdot \sum_{p \succeq o} \prod_{i=1}^{k(p)-1} \Phi_p(i) \right) \cdot D^{-n_t(o) - n_a(o) + n_i(o)} \\ &= (-1)^{n_e} \cdot B^{n_e} \cdot \sum_{p \in S(n_v)} \prod_{i=1}^{k(p)-1} \Phi_p(i) \cdot \sum_{o \preceq p} \left((-1)^{k(o)-1} \cdot D^{-n_t(o) - n_a(o) + n_i(o)} \right). \end{aligned}$$

The *reverse* \overline{p} of a surjection p is defined as follows: $\overline{p}(i) = k(p) + 1 - p(i)$. Since $C(\mathcal{S}) = C(\mathcal{S}^{\text{c}})$, $\prod_{i=1}^{k(p)-1} \Phi_p(i) = \prod_{i=1}^{k(\overline{p})-1} \Phi_{\overline{p}}(i)$. As a consequence:

$$\overline{R}_s^b = (-1)^{n_e} \cdot B^{n_e} \cdot \sum_{p \in S(n_v)} \prod_{i=1}^{k(\overline{p})-1} \Phi_{\overline{p}}(i) \cdot \sum_{o \preceq p} \left((-1)^{k(o)-1} \cdot D^{-n_t(o) - n_a(o) + n_i(o)} \right)$$

We apply the change of variable $p \rightarrow \overline{p}$:

$$\overline{R}_s^b = (-1)^{n_e} \cdot B^{n_e} \cdot \sum_{p \in S(n_v)} \prod_{i=1}^{k(p)-1} \Phi_p(i) \cdot \sum_{o \preceq \overline{p}} \left((-1)^{k(o)-1} \cdot D^{-n_t(o) - n_a(o) + n_i(o)} \right).$$

To conclude that R_s^b is symmetric, it is now enough to prove that for any offset graph, and for any surjection p , the following lemma holds:

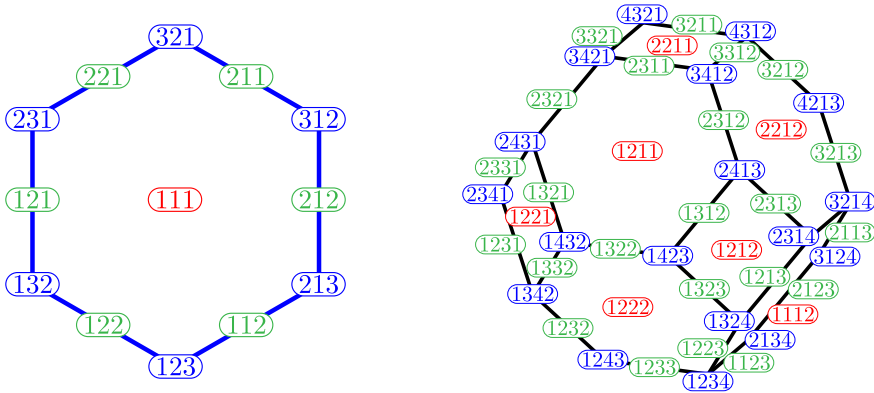


Fig. 16. Permutahedra of dimension 2 and 3. Faces of dimension 0, 1, and 2 are represented in blue, green, and red.

Lemma 5.3. For any surjection p :

$$\sum_{o \preceq \bar{p}} \left((-1)^{k(o)-1} \cdot D^{-n_t(o)-n_a(o)+n_i(o)} \right) = (-1)^{n_e} \cdot D^{n_t(p)+n_a(p)-n_i(p)}.$$

The general case of Lemma 5.3 will be proved in Section 5.3.

Remark 5.2. Note that, when the offset graph is empty, this formula can be obtained as a direct byproduct of the Euler–Poincaré formula applied to the permutahedron. The n -permutahedron (see Fig. 16) is a polytope defined as the convex hull of the set of permutations: $Perm_n = Conv\{(\sigma_1, \sigma_2 \cdots \sigma_n) \text{ such that } \sigma \in \mathfrak{S}_n\}$, where \mathfrak{S}_n is the set of permutations of size n . The n -permutahedron has dimension $n - 1$. The k -dimensional faces of the n -permutahedron correspond to surjections from $[n]$ to $[n - k]$. If $o \preceq p$, then the face corresponding to o is included into that of p .

The Euler–Poincaré formula states that, if f_k denotes the number of i -dimensional faces of a polytope, then: $\sum_{k \geq 0} (-1)^k f_k = 0$. A face of a polytope is also a polytope; in the case of the permutahedron, it is even the Cartesian product of lower-dimensional permutahedra. Therefore, the Euler–Poincaré formula applied to the face corresponding to \bar{p} implies: $\sum_{o \preceq \bar{p}} (-1)^{k(o)-1} = (-1)^{n_e}$.

5.3. Proof of Lemma 5.3

We now consider a more general context than above, with a variable X_{ij} for all $i < j$. For a surjection p of size n_v we define a monomial $X(p) = \prod_{i < j} (\delta_{p(i) > p(j)} X_{ij} + \delta_{p(i) \leq p(j)} X_{ij}^{-1})$. Note that no two permutations have the same monomial.

To a given surjection p , we associate a so-called *canonical permutation* $r(p)$ as follows:

$$r(p)(i) = |\{j \text{ such that } p(j) < p(i)\}| + |\{j \text{ such that } p(j) = p(i) \text{ and } j \geq i\}|.$$

This permutation is the linear extension of the partial order induced by p , such that each time a choice is to be made, elements are taken in decreasing order.

Lemma 5.4. *The alternated sum of monomials of surjections that refine a given surjection p is equal to the monomial of the canonical permutation of p :*

$$\sum_{o \preceq p} (-1)^{k(o)} X(o) = (-1)^{n_v} X(r(p)).$$

Proof. We group all surjections refining p that have the same monomial. For any monomial, there is exactly one such surjection that is a permutation.

Let q be a permutation that refines p . An *admissible ascent* of a permutation q is a pair of numbers $(i, i + 1)$ such that $q(i + 1) < q(i)$ and $p(i + 1) = p(i)$. The surjections that refine p and have same monomial as q are those which can be obtained from q by giving the same value to the pairs of successive numbers corresponding to some of its *admissible ascents*. The set of such surjections is therefore in bijection with the set of subsets of admissible ascents.

Consequently, except if q has no admissible ascent, the alternated sum of the ordered partitions that have the same monomial as q is 0. The only permutation that has no admissible ascent is $r(p)$, and $k(r(p)) = n_v$ (since $r(p)$ is a permutation). \square

Lemma 5.5. *For any surjection p , the following equality holds:*

$$X(r(p)) = X(\bar{p})^{-1}.$$

Proof. For $i < j$:

- If $p(i) > p(j)$, then the power of X_{ij} in $X(r(p))$ is -1 and the power of X_{ij} in $X(\bar{p})$ is 1 .
- If $p(i) \leq p(j)$, then the power of X_{ij} in $X(r(p))$ is 1 and the power of X_{ij} in $X(\bar{p})$ is -1 . \square

The following proposition is a direct consequence of Lemmas 5.4 and 5.5.

Proposition 5.6. *The reverse of the monomial associated to an ordered partition p is equal to the alternated sum of monomials associated to the ordered partitions that refine the reverse of p :*

$$X(p)^{-1} = \sum_{o \preceq \bar{p}} (-1)^{k(o) - n_v} X(o).$$

We now specialize Proposition 5.6, so as to obtain a proof of Lemma 5.3.

Proof of Lemma 5.3. Recall that the vertices have been relabeled in an order which is a linear extension of the offset graph, and by consequence any oriented edge (i, j) of the offset graph satisfies $i < j$.

We use Proposition 5.6, and specialize X_{ij} to D to a power equal to the number of oriented offset edges (i, j) . We obtain:

$$X(p)^{-1} = \sum_{o \preceq \bar{p}} (-1)^{k(o)-n_v} X(o)$$

$$D^{n_t(p)+n_a(p)-n_i(p)} = \sum_{o \preceq \bar{p}} (-1)^{k(o)-n_v} \cdot D^{-n_t(o)-n_a(o)+n_i(o)}.$$

The Euler formula applied to a scheme states that $n_v - n_e = 1 - 2g$ and by consequence $(-1)^{n_v} = (-1)^{n_e+1}$, which conclude the proof. \square

6. Opening non-bicolorable maps

In this section, we extend the opening bijection (Theorem 3.14) to general maps (not necessarily bicolorable), by considering fractional orientation. This generalization is based on the work of Bouttier, di Francesco and Guitter in [11], that was later revisited by Albenque and Poulalhon in [1].

We proved in Theorem 3.14 that the opening algorithm, applied to bicolorable maps with dual-geodesic orientation, is actually a bijection with a certain family of unicellular blossoming maps (namely \mathcal{O}). However, if the map is non-bicolorable, it is not possible to define its dual-geodesic orientation, because some adjacent faces may be at the same distances from the root face. Fractional orientation allow to deal with the case of adjacent faces with the same label.

We define the *face-doubled* (resp. *vertex-doubled*) version of a map m , denoted m^{\parallel} (resp. m^{\dagger}), as the map m where each edge is replaced by 2 adjacent copies of the edge (resp. divided into 2 parts by adding a new vertex in the midst of it). The faces (resp. vertices) hereby created are called *edge-faces* (resp. *edge-vertices*). Note that these are dual notions, so that $(m^{\parallel})^* = (m^*)^{\dagger}$, and that m^{\parallel} is bicolorable, while m^{\dagger} is bipartite. A *face-doubled orientation* (resp. *vertex-doubled orientation*) of a map m is an orientation of m^{\parallel} (resp. m^{\dagger}), with the additional constraint that no edge-face (resp. edge-vertex) is clockwise (resp. a sink).

The *geodesic doubled-orientation* (resp. *dual-geodesic doubled-orientation*) of a map m is the vertex-doubled (resp. face-doubled) orientation of m corresponding to the geodesic (resp. dual-geodesic) orientation of the bipartite map m^{\dagger} (resp. the bicolorable map m^{\parallel}).

These orientations of the doubled map can alternatively be seen as *fractional orientations* of the original map. This means that for each edge of the map, instead of choosing either one orientation of the edge or the other, we choose a fractional combination of the 2. In particular, we use *half-orientations*, which means that each edge is either oriented in one direction, or in both, in which case it is called *bi-oriented*. Note that half-orientations of a map are in bijection with doubled orientations of the doubled version of the map. A half-orientation is called *bipartite* (resp. *bicolorable*) if its corresponding orientation in the vertex-doubled (resp. face-doubled) map is bipartite (resp. bicolorable).

Note that the geodesic half-orientation is bipartite. It can alternatively be defined by labeling all vertices by their distance to the root, and orienting each edge according to the labels of its adjacent vertices: toward the vertex with smaller label if the labels are different, or bi-oriented if the labels are equal.

The work of Propp can perfectly be applied to orientations of the doubled version of a map. Note however that the resulting lattice will contain orientations that are not doubled orientations, but that by definition, the minimum of the lattice will necessarily correspond to a doubled orientation, which makes it possible to transcribe it back to a fractional orientation of the original map.

Theorem 6.1 (Propp). *The transitive closure of the vertex-push (resp. face-flip) operation endows the set of bipartite (resp. bicolorable) orientations of the vertex-doubled (resp. face-doubled) version of a fixed map with a structure of distributive lattice, whose minimum is a vertex-doubled (resp. face-doubled) orientation, namely the geodesic (resp. dual-geodesic) doubled orientation.*

A face of a map with a fractional orientation is called *clockwise* if it has no edge oriented completely counterclockwise. Theorem 6.1 leads to Corollary 6.2:

Corollary 6.2. *The dual-geodesic half-orientation of a map is the unique bicolorable half-orientation of this map with no clockwise face other than the root face.*

Algorithm 3 The fractional opening algorithm.

Input: A map m embedded on a surface \mathcal{S} , rooted at a corner c_0 , along with a half-orientation.

Output: A half-oriented blossoming embedded graph $b = \text{open}(m)$, embedded on \mathcal{S} .

Set $c = c_0$, $b = \emptyset$, and $E_V = \emptyset$ (E_V is the set of visited edges).

repeat

$e = \text{NE}(c)$.

 if $e \notin E_V$ and e is oriented toward $\text{vertex}(c)$ or bi-oriented then

 add e to E_V

 add e to b

$c \leftarrow \text{NaF}(c)$

 else if $e \notin E_V$ and e is fully outgoing from $\text{vertex}(c)$ then

 add e to E_V

 Add a bud to b in place of e .

$c \leftarrow \text{NaV}(c)$

 else if $e \in E_V$ and e is fully oriented toward $\text{vertex}(c)$ then

 Add a leaf to b in place of e .

$c \leftarrow \text{NaV}(c)$

 else if $e \in E_V$ and e is outgoing from $\text{vertex}(c)$ or bioriented then

$c \leftarrow \text{NaF}(c)$

 end if

until $c = c_0$

We now redefine the opening algorithm (see Algorithm 3), by always considering that a bi-oriented edge is visited backward first. This roughly amounts to applying the classical opening algorithm to the face-doubled version of the map. Note that this algorithm can still be seen as the dual of a tour of a breadth-first-search exploration tree. The closing algorithm remains the same.

We redefine some properties to match fractional orientations. A unicellular map is called *well-half-oriented* if, in a tour of the face, the first occurrence of any edge is either oriented backward or bi-oriented. The definition of a *well-labeled* map is the same, with the additional rule that the labels of corners adjacent around a vertex and separated by a bi-oriented edge have to be equal.

The set of well-rooted well-labeled well-half-oriented blossoming unicellular maps, is denoted \mathcal{OG} . We count maps of \mathcal{M} and \mathcal{OG} by vertex degrees of any parity (unlike bicolourable maps, that we counted earlier only by even vertex degrees), so that for instance $M(\mathbf{z}) = M(z_1, z_2, \dots) = \sum_{m \in \mathcal{M}} \prod_{k=1}^{\infty} z_k^{v_k(m)}$.

We now state the generalization of Theorem 3.14 to general maps.

Theorem 6.3. *The opening algorithm on a dual-geodesically half-oriented map is a weight-preserving bijection from \mathcal{M}_g to \mathcal{OG}_g , whose reverse is the closing algorithm. Therefore, $M_g(\mathbf{z}) = OG_g(\mathbf{z})$.*

Remark 6.1. This result looks similar to Corollary 3.15. However, the bijection leading to Corollary 3.15 is really from 4-valent bicolourable maps (to some blossoming maps), rather than from general maps. Although we were able, using Corollary 3.15 in conjunction with Proposition 2.10, to obtain rich enumerative and structural results on general maps, the bijection as it stands cannot be specialized to control the degree of faces, for instance.

In contrast, the bijection introduced in Section 6, is an opening bijection for general maps, and allows such specialization. It could be a starting point to obtaining further more precise result on the structure of general maps, as it was the case for planar maps [11].

Acknowledgments

I would like to thank my supervisors Marie Albenque and Vincent Pilaud for many discussions about both the content and presentation of the present work.

I also thank Guillaume Chapuy, Gilles Schaeffer, and Éric Fusy for insightful discussion about their own work and the general state of the art.

I finally thank the reviewers for their fruitful remarks on the paper.

My work was partially supported by the project ANR-16-CE40-0009.

References

- [1] M. Albenque, D. Poulalhon, A generic method for bijections between blossoming trees and planar maps, *Electron. J. Combin.* 22 (2) (2015) P2-38.
- [2] E.A. Bender, E.R. Canfield, The number of rooted maps on an orientable surface, *J. Combin. Theory Ser. B* 7 (1) (1991) 9–15, <https://doi.org/10.1137/S0895480190177650>.
- [3] A.E. Bender, E.R. Canfield, L.B. Richmond, The asymptotic number of rooted maps on a surface: II. Enumeration by vertices and faces, *J. Combin. Theory Ser. A* 63 (2) (1993) 318–329, [https://doi.org/10.1016/0097-3165\(93\)90063-E](https://doi.org/10.1016/0097-3165(93)90063-E).

- [4] E.A. Bender, E. Rodney Canfield, R.W. Robinson, The asymptotic number of tree-rooted maps on a surface, *J. Combin. Theory Ser. A* 48 (2) (1988) 156–164, [https://doi.org/10.1016/0097-3165\(88\)90002-7](https://doi.org/10.1016/0097-3165(88)90002-7).
- [5] O. Bernardi, Bijective counting of tree-rooted maps and shuffles of parenthesis systems, *Electron. J. Combin.* 14 (1 R) (2006) 1–36.
- [6] O. Bernardi, G. Chapuy, A bijection for covered maps, or a shortcut between Harer–Zagier’s and Jackson’s formulas, *J. Combin. Theory Ser. A* 118 (6) (2011) 1718–1748, <https://doi.org/10.1016/j.jcta.2011.02.006>.
- [7] O. Bernardi, É. Fusy, A bijection for triangulations, quadrangulations, pentagulations, etc, *J. Combin. Theory Ser. A* 119 (1) (2012) 218–244, <https://doi.org/10.1016/j.jcta.2011.08.006>.
- [8] O. Bernardi, É. Fusy, Unified bijections for maps with prescribed degrees and girth, *J. Combin. Theory Ser. A* 119 (6) (2012) 1351–1387, <https://doi.org/10.1016/j.jcta.2012.03.007>.
- [9] J. Bettinelli, A bijection for nonorientable general maps, in: *Canada DMTCs Proc. BC*, 2016, pp. 227–238.
- [10] N. Bonichon, B. Lévêque, A bijection for essentially 4-connected toroidal triangulations, Manuscript, arXiv:1707.08191.
- [11] J. Bouttier, P. Di Francesco, E. Guitter, Census of planar maps: from the one-matrix model solution to a combinatorial proof, *Nuclear Phys. B* 645 (3) (2002) 477–499, [https://doi.org/10.1016/S0550-3213\(02\)00813-1](https://doi.org/10.1016/S0550-3213(02)00813-1).
- [12] J. Bouttier, P. Di Francesco, E. Guitter, Planar maps as labeled mobiles, *Electron. J. Combin.* 11 (1 R) (2004) 1–27.
- [13] S.R. Carrell, G. Chapuy, Simple recurrence formulas to count maps on orientable surfaces, arXiv:1402.6300.
- [14] G. Chapuy, Asymptotic enumeration of constellations and related families of maps on orientable surfaces, *Combin. Probab. Comput.* 18 (4) (2009) 477–516.
- [15] G. Chapuy, M. Dolgga, A bijection for rooted maps on general surfaces, *J. Combin. Theory Ser. A* 145 (3) (2017) 252–307, <https://doi.org/10.1016/j.jcta.2016.08.001>.
- [16] G. Chapuy, M. Marcus, G. Schaeffer, A bijection for rooted maps on orientable surfaces, *SIAM J. Discrete Math.* 23 (3) (2009) 1587–1611, <https://doi.org/10.1137/080720097>.
- [17] R. Cori, B. Vauquelin, Planar maps are well labeled trees, *Canad. J. Math.* 33 (5) (1981) 1023–1042, <https://doi.org/10.4153/CJM-1981-078-2>.
- [18] V. Despré, D. Gonçalves, B. Lévêque, Encoding toroidal triangulations, *Discrete Comput. Geom.* 57 (3) (2017) 507–544, <https://doi.org/10.1007/s00454-016-9832-0>.
- [19] B. Eynard, *Counting Surfaces*, Progress in Mathematical Physics, vol. 70, Springer, 2011.
- [20] S. Felsner, Lattice structures from planar graphs, *Electron. J. Combin.* 11 (1) (2004) 15.
- [21] S. Felsner, K.B. Knauer, ULD-lattices and Δ -bonds, *Combin. Probab. Comput.* 18 (5) (2009) 707–724, <https://doi.org/10.1017/S0963548309010001>.
- [22] P. Flajolet, R. Sedgewick, *Analytic Combinatorics*, Cambridge University Press, Cambridge, 2009.
- [23] D. Gonçalves, K. Knauer, B. Lévêque, On the structure of Schnyder woods on orientable surfaces, arXiv:1501.05475v2.
- [24] S.K. Lando, A.K. Zvonkin, *Graphs on Surfaces and Their Applications*, Springer, 2004, Appendix by Don B. Zagier.
- [25] G. Miermont, Tessellations of random maps of arbitrary genus, *Ann. Sci. Éc. Norm. Supér.* 42 (5) (2009) 725–781.
- [26] D. Poulalhon, G. Schaeffer, Optimal coding and sampling of triangulations, *Algorithmica* 46 (3–4) (2006) 505–527, <https://doi.org/10.1007/s00453-006-0114-8>.
- [27] J. Propp, Lattice structure for orientations of graphs, arXiv:math/0209005, 1993.
- [28] G. Schaeffer, Bijective census and random generation of Eulerian planar maps with prescribed vertex degrees, *Electron. J. Combin.* 4 (1 R) (1997) 1–14.
- [29] G. Schaeffer, *Conjugaison d’arbres et cartes combinatoires aléatoires*, Ph.D. thesis, Université Bordeaux I, 1998.
- [30] W.T. Tutte, A census of planar maps, *Canad. J. Math.* 15 (i) (1963) 249–271, <https://doi.org/10.4153/CJM-1963-029-x>.